Applied Mathematics & Information Sciences
An International Journal

http://dx.doi.org/10.18576/amis/180615

A Deep Learning Prediction Model to Predict Sustainable Development in Saudi Arabia

Fahad Aljuaydi [1,*], *Bikash K. Behera* [2], *Ahmed M. Elshewey*[3], *and Zahraa Tarek* [4]

[1]Department of Mathematics, College of Science and Humanities, Prince Sattam bin Abdulaziz University, Al-Kharj, Saudi Arabia
[2]Department of Physical Sciences, Indian Institute of Science Education and Research Kolkata, Mohanpur 741246, West Bengal, India
[3]Department of Computer Science, Faculty of Computers and Information, Suez University, P.O.BOX:43221, Suez, Egypt
[4]Department of Computer Science, Faculty of Computers and Information, Mansoura University, Mansoura 35561, Egypt

Received: 25 Feb. 2024, Revised: 30 Jun. 2024, Accepted: 10 Jul. 2024
Published online: 1 Sep. 2024

Abstract: This paper introduces a novel deep learning model specifically designed for predicting climate change in Saudi Arabia until the year 2030. The proposed model, called CNN-BRNN, is a hybrid architecture that integrates the strengths of Bidirectional Recurrent Neural Network (BRNN) and Conventional Neural Network (CNN) models. The model is employed to provide accurate predictions for four key factors: temperature, air temperature dew point, visibility distance, and air pressure at sea level. Each of these factors is individually predicted to analyze the climate change trends in Saudi Arabia up to 2030. The CNN-BRNN model is compared to five other machine learning regressors: Random Forest, Support Vector, K-Nearest Neighbor, Gradient Boosting, and Dummy regressor. The outcomes demonstrate that the CNN-BRNN model performs better than the other models. The predictions generated by the CNN-BRNN model reveal several significant climate change trends projected for Saudi Arabia until 2030. These trends include a projected 20-degree increase in the temperature, a rise in air temperature dew point, abnormal reduction in air visibility distance, and decreased air pressure at sea level. These findings highlight the potential impacts of climate change on Saudi Arabia's environment. Building upon the obtained results, decision-makers can successfully handle the challenges caused by climate change, guaranteeing the nation's sustainability in the future.

Keywords: Sustainability, SDG 12, SDG 13, Deep learning

1 Introduction

Climate change presents an urgent and significant threat, causing widespread harm to both natural and urban environments and resulting in global economic losses surpassing 500 billion [1]. Both quantum computing [2,3] and classical computing systems push AI to provide a partial solution by utilizing online resources [4,5] to deliver timely recommendations derived from accurate climate change forecasts. The versatility of AI extends to various applications aimed at mitigating climate change's adverse effects, such as improving energy efficiency [6], carbon sequestration and storage [7], predicting renewable energy [8], managing power grids [9], designing sustainable buildings [10], optimizing transportation systems [11], enhancing smart agriculture [12], optimizing industrial procedures [13], decreasing deforestation [14], and creating resilient cities [15]. In this study, we thoroughly address the main problem which revolves around the urgent and significant threat posed by climate change. We highlight the widespread harm caused to both natural and urban environments, along with the substantial economic losses exceeding billions of dollars. We emphasize the critical need for effective solutions to mitigate the negative effects of climate change and fulfill the objectives of sustainable development. Moreover, we underscore the role of artificial intelligence (AI) in providing timely recommendations based on precise climate change forecasts, thereby offering partial solutions to this complex problem. By delving into various applications of AI in mitigating climate change impacts, such as improving energy efficiency, managing power grids, and optimizing transportation systems, we illustrate the broad scope of AI's potential contributions in this domain. We also discuss the challenges associated with predicting climate patterns, including data

* Corresponding author e-mail: f.aljuaydi@psau.edu.sa

availability constraints, and highlight the role of machine learning techniques in addressing these challenges.

Researchers have discovered that improving the efficiency of energy can significantly help lessen the impact of climate change [16,17,18]. Smart manufacturing has the capacity to reduce waste, energy usage, and carbon emissions by 30–50% [19]. Moreover, AI's integration in the natural gas sector, improving weather prediction accuracy by approximately 70%, underscores its potential in enhancing climate-related forecasting [20]. Integrating intelligent power grids with AI has the capacity to increase efficacy of power systems, leading to a reduction in costs of electricity by around 10–20%. Intelligent transportation systems have the potential to decrease carbon emissions by around 60% [21]. Furthermore, AI's role extends beyond mitigation efforts; it plays a vital role in fostering sustainability by streamlining natural resource management and bolstering the resilience of vulnerable areas [23]. According to the 2018 international report on climate change, annual emissions of greenhouse gases from the globe are still rising, threatening severe consequences unless addressed within a 30-year timeframe. This necessitates both mitigation efforts, focusing on emission reduction, and adaptation strategies, preparing for inevitable climate-related challenges [1]. Adaptation necessitates strategic preparation for the capacity to endure and successfully address climate-related difficulties and catastrophic incidents [24]. AI emerges as a valuable tool in both mitigating and adapting to climate change, aiding in flood and drought hazard mitigation and supporting adaptation measures such as crop monitoring for enhanced food security [25]. From an adaptation perspective, remote sensing methods for climate prediction may be utilized to monitor crops and anticipate yields, therefore enhancing food security in the presence of droughts and other severe weather conditions [26]. The challenges in predicting climate patterns are often compounded by insufficient data availability, hindering accurate forecasting. AI, particularly machine learning, aims to address by identifying and leveraging connections between climatic variables. Using pattern identification and feature extraction techniques may enable us to discern more valuable correlations within the climate system, while regression models might help us quantify non-linear associations between interconnected variables [27].

The problem addressed in this paper is to provide sustainable development for sustainability indictors based on predicting climate change. Meeting current demands is referred to as sustainable development while ensuring that future generations can also meet their own demands. It entails weighing the effects of decisions on the environment, society, and economy in order to make long-term well-being-promoting choices. Governments and legislators require scientific predictions of climate change to design effective plans and enact laws that mitigate the consequences of climate change and fulfill the objectives of sustainable development [28,29,30]. Machine learning (ML) can be extremely important for supplying future information about natural problems, including climate change. By employing ML techniques such as optimizers and ensemble regression models, promising outcomes can be achieved in forecasting the future of climate change factors [31]. Several prediction-related factors are considered when anticipating climate change, including temperature, air temperature dew point, visibility distance, and air pressure at sea level. These factors have significant implications for various sectors, such as agriculture, flooding, dense fog, shipping, aviation, transportation, tourism, and public safety [31,32].

This paper contributes to the ongoing efforts in adaptation and mitigation of climate change by leveraging machine learning and deep learning methods to predict climate changes and impacts on the development of sustainable development. Building upon the recognized potential of AI in addressing climate-related challenges across various sectors, this study focuses on integrating a diverse set of ocean-atmospheric factors into predictive models. Specifically, it employs a hybrid Bidirectional Recurrent Neural Network (BRNN) and Conventional Neural Network (CNN) model trained on key climate variables including temperature, air temperature dew point, visibility distance, and air pressure at sea level. The methodology involves rigorous evaluation using standard metrics such as MAE, RMSE, MedAE, MSE, and R2, alongside a comparative analysis of five ML regressors, namely the Gradient Boosting (GB), Random Forest (RF), Nearest Neighbor (KNN), Support Vector Regressor (SVR), and Dummy Regressor (DR). The application of the CNN-BRNN model for forecasting future climate predictions up to 2030 in Saudi Arabia further underscores its practical utility. The proposed method introduces several significant advancements, which can be listed as follows: 1. Integration of Diverse Ocean-Atmospheric Factors: The study incorporates a wide range of ocean-atmospheric factors, including temperature, air temperature dew point, visibility distance, and air pressure at sea level, into predictive models, enhancing the comprehensiveness of climate change forecasting. 2. Hybrid CNN-BRNN Model: Introducing a novel hybrid model combining BRNN and CNN architectures, which effectively captures temporal dependencies and spatial correlations in climate data, leading to improved prediction accuracy. 3. Comprehensive Evaluation and Comparison: Rigorous evaluation of the proposed model using standard metrics such as MAE, RMSE, MedAE, MSE, and R2, alongside a comparative analysis with five commonly used machine learning algorithms, providing robust validation of its performance. 4. Long-Term Climate Prediction: Application of the CNN-BRNN model to forecast future climate predictions up to 2030 in Saudi Arabia, offering valuable insights into long-term climate trends and

facilitating proactive planning and decision-making. The structure of the paper is as follows: The review of the literature is summarized in Section 2. Section 3 outlines the methods used and the model development process. Section 5 presents the findings and room for more investigation, whereas Section 4 discusses the results.

2 Literature review

Recent research explores the nexus of environmental sustainability, urban resilience, and predictive modeling. Supervised machine learning segmentation aids coastal region management [33], complementing AI applications in stormwater infrastructure for smart cities [34]. Sustainable development studies, like Uruguay's environmental policies amidst globalization [35], align with renewable energy analyses, such as seasonal solar system usage in Iran [36]. Predictive modeling advancements, integrating neural architectures with linear regression for traffic predicting [37], parallel investigations into urban infrastructure vulnerabilities, like small-scale storm sewer geysers [38]. For climate change prediction, various predicting issues can be considered, e.g., temperature, sea level pressure, visibility, and dew predictions. This section discusses some of the studies focused on these issues. S.P. Nitsure et al. [39] utilized Artificial Neural Network (ANN) and Genetic Programming (GP) methods to forecast sea levels indirectly. They achieved this by anticipating sea level anomalies (SLAs) utilizing the hourly-collected local wind shear velocity ingredients as inputs from the specific time to the preceding 12 hours. The investigation was carried out at four locations situated in close proximity to the shoreline of the United States. The predictions made by the GP algorithm are superior to those made by the ANN algorithm. The study yielded a maximum correlation coefficient of 0.998, MAE of 0.106 m, a scatter index (SI) of 0.031, and a coefficient of efficiency (CE) of 0.995 for 1-day GP predictions. Rifat Tur et al. [40] developed methodology for predicting fluctuations in sea levels by utilizing data from sea level elevation measurements and meteorological parameters gathered from a tidal gauge located in Turkey. Multiple prediction models were constructed utilizing adaptive neuro-fuzzy inference system and linear regressions methods. The results demonstrated that using meteorological factors as input variables greatly improved the computational accuracy of the MLR methods by up to 33% in predicting short-term sea levels. Furthermore, the findings provided a more accurate comprehension that ANFIS outperformed MLR in predicting sea level utilizing lagged sea level observations (SC1), as well as combined meteoro logical variables observations and lagged sea level (SC2) as input combinations. Tayeb Brahimi [28] suggested employing the ANNs technique to forecast the daily wind speed throughout several regions in Saudi Arabia. The proposed approach is a feed-forward NN algorithm with the back-propagation method for supervised learning. The findings revealed that the optimal configuration is achieved by employing 30 neurons in the hidden layers, which corresponds to the lowest RMSE and the maximum R. An analysis of five ML methods, including Random Forest (RF), Random Tree (RT), ANN, Support Vector Machines (SVM), and RepTree, showed that RT has a small correlation and a highly significant root mean square error. Mohammed Baljon et al. [41] outlined the essential features necessary for forecasting precipitation. They employed the ML technique as a novel classification method to evaluate whether the anticipated rainfall would be moderate or intense.

The performance measures are considered using several metrics, including RMSE, accuracy, MAE, recall, error, and F-measure. The results demonstrated that Function Fitting Artificial Neural Network classifier (FFANN) outperformed other classification techniques. The DT algorithm accomplished a 96.1% success rate, surpassing the RF classifier by 2.22 %, the KNN classifier by 7.3%, the SVM classifier by 4.99%, the ANN classifier by 4%, and the MLR classifier by 13.33%. Authors in [42] tested 36 Regressors for forecasting the indoor temperature in an intelligent building for three straight hours. The comparison was based on real data gathered every ten minutes from both a weather station and a smart building. The models utilized in machine learning are Random Forest, Gradient Boosting Machine, and Extra Trees. RMSE and R were used to evaluate the models. According to the findings, the Extra Trees had a smaller RMSE of 0.058 and a higher correlation value of 0.97. An investigation by three ML regressors was used in research by [43] to forecast daily rainfall in Ethiopia from 1999 to 2018 using RF, XGBoost, and MLR.

The weather station provided a dataset with several characteristics including rainfall, evaporation, maximum temperature, lowest temperature, humidity, sunshine, wind speed, date, month, and year. For MLR, RF, and XGBoost, the Mean Absolute Error (MAE) values are respectively, 4.97, 4.49, and 3.58. For RF, MLR, and XGBoost, the corresponding RMSE values are 8.61, 8.82, and 7.85. Chimango Nyasulu et al. [44] conducted a Comparative analysis of 10 ML Regressors and a suggested Ensemble Approach. The Ensemble Model outperformed the ten basic models, according to the experimental results. The following were the Ensemble Model findings for each parameter: The MAE, RMSE, MSE, and R for relative humidity were 4.0126, 29.9885, 5.4428, and 0.9335, respectively. The MAE, RMSE, MSE, and R for the minimum temperature were, respectively, 0.7908, 1.0515, 1.1329, and 0.9018. The MAE, MSE, RMSE, and R for maximum temperature were 1.2515, 2.8038, 1.6591 and 0.8205. For rainfall, the coefficient of determination was 0.7733, the MAE was 0.2142, the MSE was 0.1681, and the RMSE was 0.4100. The results demonstrated that the Ensemble Model can be utilized to anticipate maximum and minimum temperatures, relative humidity, and rainfall. Therefore, it

can be shown from the literature on ocean and atmospheric research that no work has been done on temperature, sea level pressure, visibility, or dew forecast in the same dataset.

Thus, there is a scope for exploring CNN and BRNN in order to improve the precision of temperature, air temperature dew point, visibility distance, and air pressure at sea level predictions utilizing the main causative factors.

3 Problem Statement and Methodology

The problem addressed in this study is the urgent need for sustainable development procedures amidst the escalating challenges of climate change. Both human societies and natural ecosystems are seriously threatened by climate change, leading to widespread environmental degradation, economic losses, and social disruptions. To combat this pressing issue, effective policies are needed to reduce the effects of climate change while promoting long-term well-being and resilience. However, designing such strategies necessitates accurate predictions of future climate changes and their implications. This study focuses on leveraging ML and DL methods to improve predictive models capable of forecasting key climate variables. By integrating a wide range of ocean-atmospheric factors and employing advanced modeling techniques, the aim is to provide decision-makers with actionable insights for formulating sustainable development policies and adaptation measures. The proposed framework for climate change prediction in the first phase is described in Figure 1.

This paper's primary objective is to investigate the influence of sustainability development based on predicted changes in atmospheric and oceanic factors resulting from climate change, specifically focusing on four factors: temperature, air temperature dew point, visibility distance, and air pressure at sea level. This objective is accomplished in two phases. In the first phase, five traditional machine learning models (RF, KNN, SVR, GB, and DR) and a deep learning model (CNN-BRNN) are trained using two datasets to predict the four identified factors. The CNN-BRNN model combine the CNN and BRNN models. Performance evaluation metrics are used to assess the models, and the outcomes demonstrate that the CNN-BRNN model performs better than the traditional ones in all four factors. In the second phase, because the CNN-BRNN model outperforms the other five traditional machine learning models, it is then utilized to predict four climate predictions. The first scenario involves forecasting the temperature for the period of May 2019 to May 2030 in SAUDI ARABIA. The second scenario focuses on predicting the temperature dew point for the same time frame in Saudi Arabia. The third scenario aims to forecast the visibility distance, while the final scenario concentrates on predicting the sea level pressure, all spanning May 2019 to May 2030 in SAUDI ARABIA. The subsequent subsections provide a detailed description of the proposed methodology.

Table 1: The Statistical analysis of first dataset.

Attributes	mean	min	std	max
year	2017.7100	2017.0	0.7061	2019.0
month	6.0507	1.0	3.5216	12.0
day	15.6911	1.0	8.788	31.0
hour	12.5369	1.0	6.9103	24.0
minute	0.1311	0.0	1.9707	59.0
temp	24.723	-4.0	8.8809	50.0
wind	12.9571	-1.0	8.7116	163.0
barometer	1015.4554	904.0	6.9708	1101.0
visibility	11.053453	-1.0	7.0530	161.0

3.1 Dataset Description

We used two datasets- the first one is utilized to predict temperature in SAUDI ARABIA for ten years, and the second one is employed to predict wind speed, sea level pressure, visibility, and dew. The first dataset is available at: https://www.kaggle.com/datasets/esraamadi/saudi-arabia-weather-history, with 249023 instances and 14 features. The second dataset is available at: https://datasource.kapsarc.org/explore/dataset/saudi-hourly-weather-data/information/. The second dataset contains 15 Governorates with 1048574 instances and 23 features. The two datasets are divided into 70% for training set, 15% for validation set to tune the hyperparameters, and 15% for testing set to evaluate the model's performance. For the first dataset, the number of instances for training is 174,317, for validation is 37,353, and for testing is $37,353$. For the second dataset, the number of instances for training is $734,002$, for validation is 157,286, and for testing is $157,286$. The statistica analysis and heat map of the first dataset are described in Figure 2 and Table 1. Additionally, the statistical analysis and heat map of the second dataset are represented in Figure 3 and Table 2. Heat map analysis is an essential tool for analyzing and visualizing data, especially when dealing with large data sets with many features. Here are several reasons why heatmap analysis is important for analyzing data set features. Heat maps are excellent for visualizing the correlation between different features in a data set. By representing correlations through color gradients, heat maps can quickly show which features are positively or negatively correlated, which is critical for understanding relationships within data. Trends and patterns that might not be immediately obvious from raw data can be revealed on heat maps. By displaying the data in a matrix format, it becomes easier to see clusters or clusters of attributes with similar behaviors. It is easy to

Table 2: The Statistical analysis of first dataset.

Attributes	mean	min	std	max
Wind Direction Angle	277.1818	229.74	180.0	999.0
Wind Speed Rate	35.54949	171.37	0.0	999.9
Sky Ceiling Height	45855.23	37878	3600.0	9999
Visibility Distance	20425.24	99457	9900.0	9999
Air Temperature Dew Point	58.1697	218.31	1.7	999.9
Air Temperature	63.56969	217.06	7.0	999.9
Atmospheric Sea Level Pressure	9908.5	909.31	952.3	9999

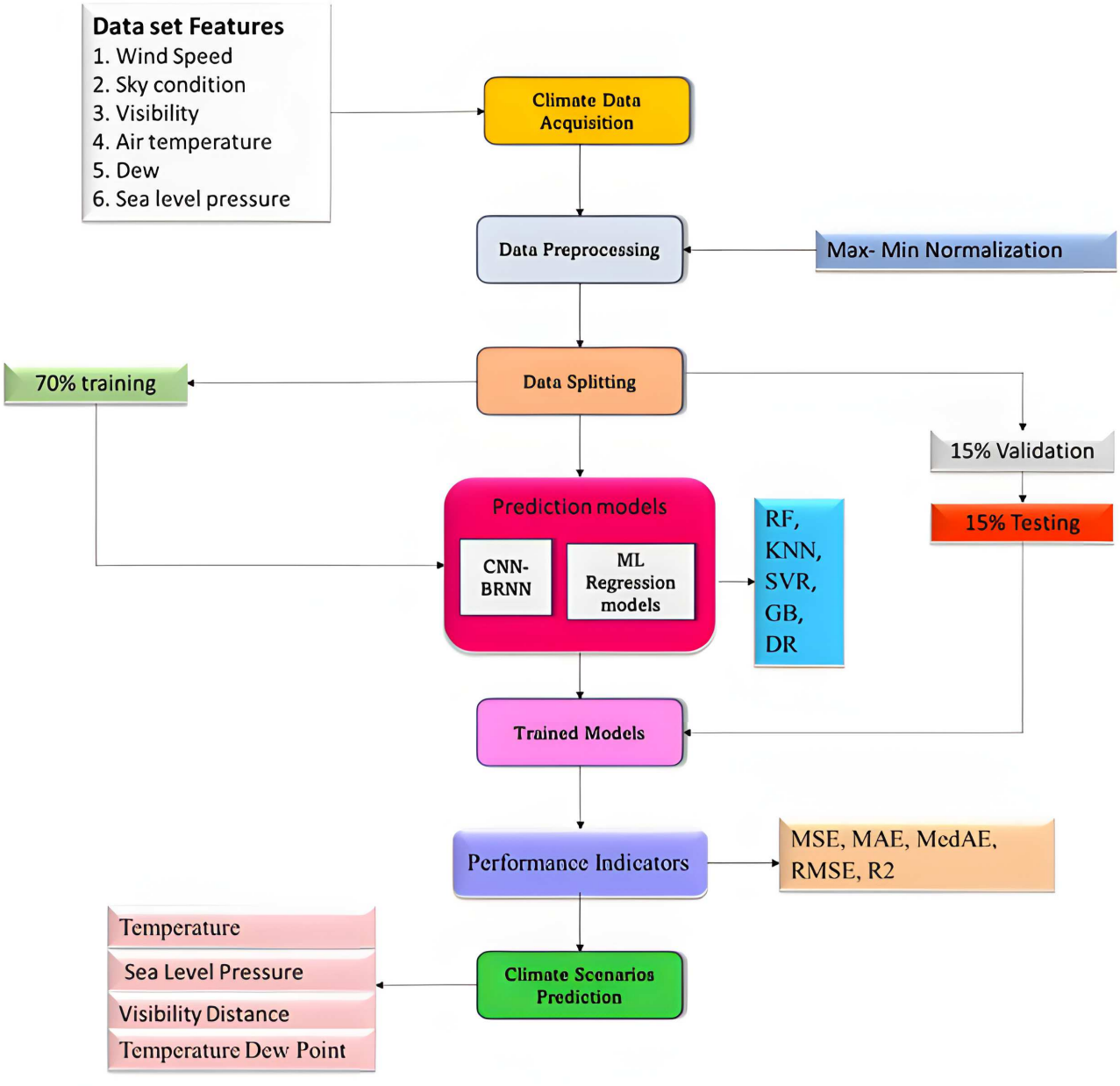

Fig. 1: Proposed Framework for Climate Change Prediction in Saudi Arabia.

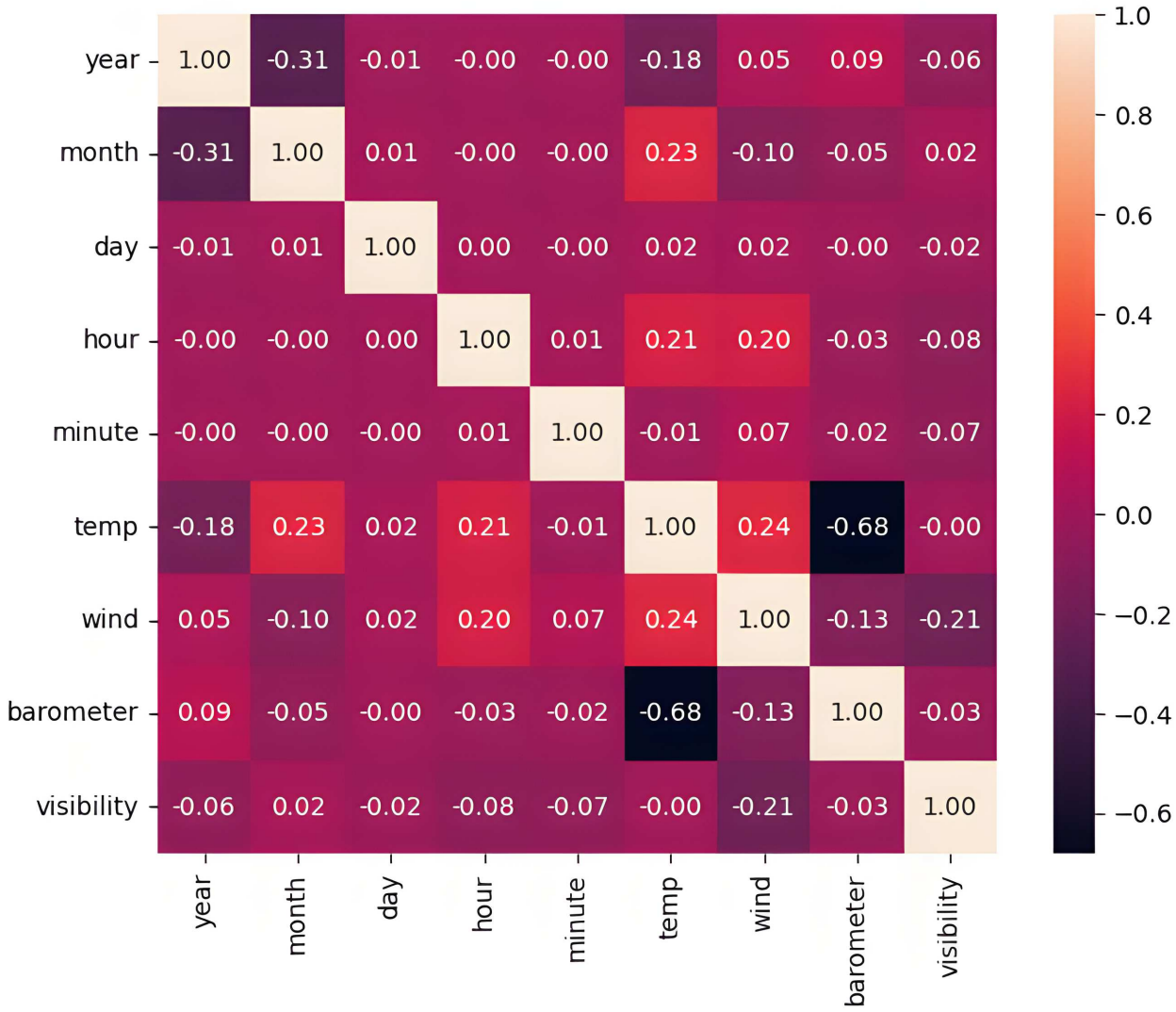

Fig. 2: Heat Map of the First Dataset's Ocean and Atmosphere Parameter Correlation Matrix.

spot outliers or anomalies in a heat map due to distinct color differences. This is important to clean the data and ensure the quality of the dataset before further analysis. Heatmaps can aid in feature selection by showing features that have strong associations with the target variable. This helps build more efficient and accurate predictive models by focusing on the most relevant attributes [56,37]. Figure 2 shows a heat map matrix, that shows the correlation between the first dataset features. In this case, the features are minute, hour, day, month, year, wind speed, temperature, barometer, and visibility. The correlation coefficient between two features varies between -1 and 1. A perfect positive correlation is represented by a correlation coefficient of 1, a perfect negative correlation is represented by -1, and no correlation is represented by 0. Some observations from the heat map matrix in Figure 2 are:

- A moderate positive correlation between temperature and barometric pressure (0.24).
- A weak negative correlation between temperature and visibility (-0.00).
- A strong positive correlation between wind speed and barometric pressure (0.13). • A weak negative correlation between wind speed and visibility (-0.21).
- A weak positive correlation between barometric pressure and visibility (0.03).

Figure 3 is a heatmap matrix, which shows the correlation between the features of the second dataset. The features are wind direction angle, wind speed rate, sky ceiling height, visibility distance, air temperature, air temperature dew point, and air pressure at sea level. Some observations from the heat map matrix in Figure 3 are:

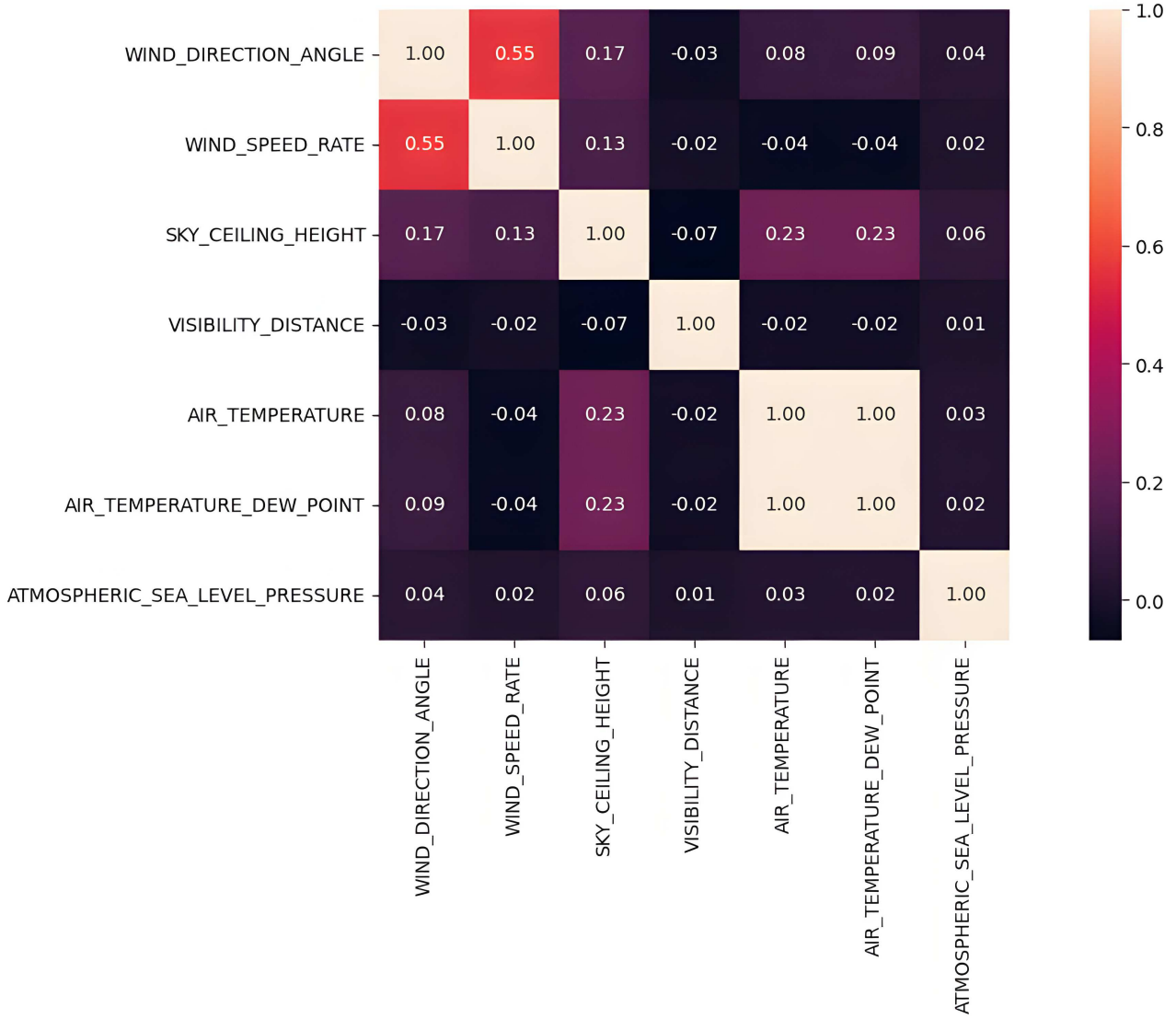

Fig. 3: Heat Map of the Second Dataset's Ocean and Atmosphere Parameter Correlation Matrix.

• Wind direction angle has a weak positive correlation with sky ceiling height (0.17).
• Wind direction angle has a weak positive correlation with atmospheric sea level pressure (0.04).
• Wind speed rate has a weak negative correlation with sky ceiling height (-0.07).
• Wind speed rate has a very weak negative correlation with visibility distance (-0.02).
• Sky ceiling height has a moderate positive correlation with air temperature (0.23).
• Sky ceiling height has a moderate positive correlation with air temperature dew point (0.23).
• Air temperature has a perfect positive correlation with air temperature dew point (1.00). This is likely because the data was collected at a single time or location, where the temperature and dew point would be very similar.
• Visibility distance has a weak positive correlation with atmospheric sea level pressure (0.01).

3.2 Min-Max Normalization

During preprocessing, the affecting factors' values are adjusted to a specified limit using the Min-Max normalization. The goal of this most basic type of normalization is to adjust every variable to lie in the interval [0,1]. Equation (1) shows that for every value in the set of observed values of x, the variable Z is modified to a new value within the interval [0,1] [45].

$$Z_i = \frac{x_i - Min}{Max - Min}.$$

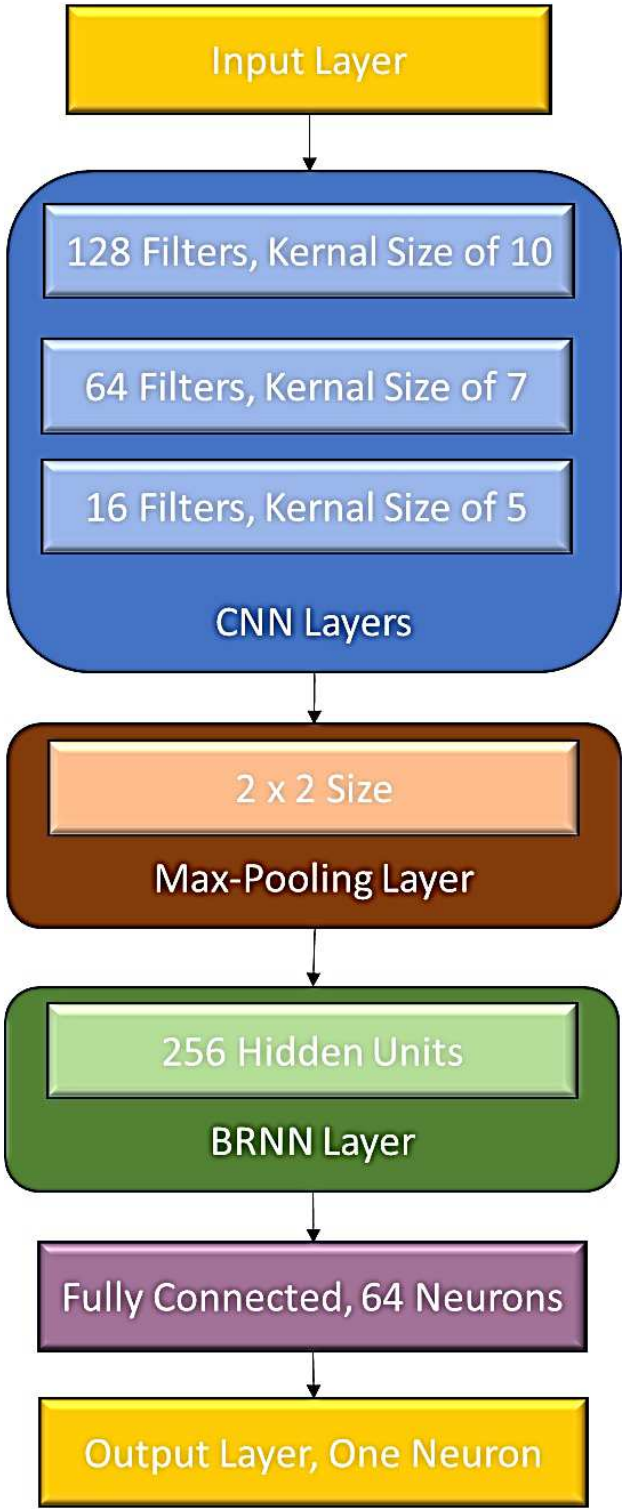

Fig. 4: Architecture of CNN-BRNN Model.

3.3 The proposed and Reference Models

3.3.1 CNN-BRNN

CNNs primarily rely on a supervised learning procedure that is motivated by the way people naturally focus on visuals. Since CNNs do not require any kind of feature extraction preparation, they are preferred over other machine learning models. CNNs belong to a class of deep neural networks that includes convolutional, non-linear activation, and max-pooling layers. One of CNN's essential layers is the convolutional layer, is where convolution is executed. Kernels are used in the convolutional layer to process the incoming data. The convolution of every and each output of the convolutional layer yields feature maps [46,47]. The process of convolution can be illustrated as illustrated in Eq. (1).

$$s(i,j) = (X * W)(i,j) + b = \sum_{k=1}^{n_{in}} (X_k * W_k(i,j) + b). \quad (1)$$

where n_{in} represents the tensor's final dimension number or input indices, Xk denotes the source index of kth, the kth sub-convolution matrix is represented by W_k, and $s(i,j)$ indicates the specific element value in the outcome matrix associated with the convolution kernel W. The Rectified Linear Unit (ReLU) function, defined as $f(x) = max(0,x)$, is frequently used to represent the non-linear layers output. ReLU function sets the value of any negative input to 0, while leaving positive values unchanged [48]. The BRNN consists of both a forward RNN and a backward RNN. The BRNN does reverse feature processing based on the sequencing data's forward feature processing. This property can comprehensively account for the bidirectional correlation between factors [49,50]. The initial input sequence data unit $x^j_{embeded_{i1}}$ was fed into the forward operation's initial RNN cell, while the final input sequence data unit $(x^j_{embeded_{i4}})$ was fed into the second RNN for the reverse operation. The output hidden layer sequence $(h^j_{i1}, h^j_{i2}, h^j_{i3}, h^j_{i4})$was created by combining the outcomes of the forward and reverse calculations. The operational procedure of BRNN was mathematically defined by Eq.(3-5).

$$h^{(}_{it} j(f)) = \tanh(W_1 x^j_{embeded_{it}} + W_2 h^j_{i(t-1)}), \quad (2)$$

$$h^{(j(b))}_{it} = \tanh(W_1 x^j_{embeded_{it}} + W_2 h^j_{i(t-1)}, \quad (3)$$

$$h^j_{it} = h^{(j(f))}_{it} \otimes h^{j(b)}_{it}. \quad (4)$$

where $\otimes$ represents the concatenation operation, $h^{(j(f))}_{it}$ and $h^{j(b)}_{it}$ indicate the hidden outputs of the tth forward and backward RNN cell. Due to the strong bidirectional dependency in the the sample data's feature sequence, it is very easy to understand the interaction between the different variables [50]. The design of CNN-BRNN

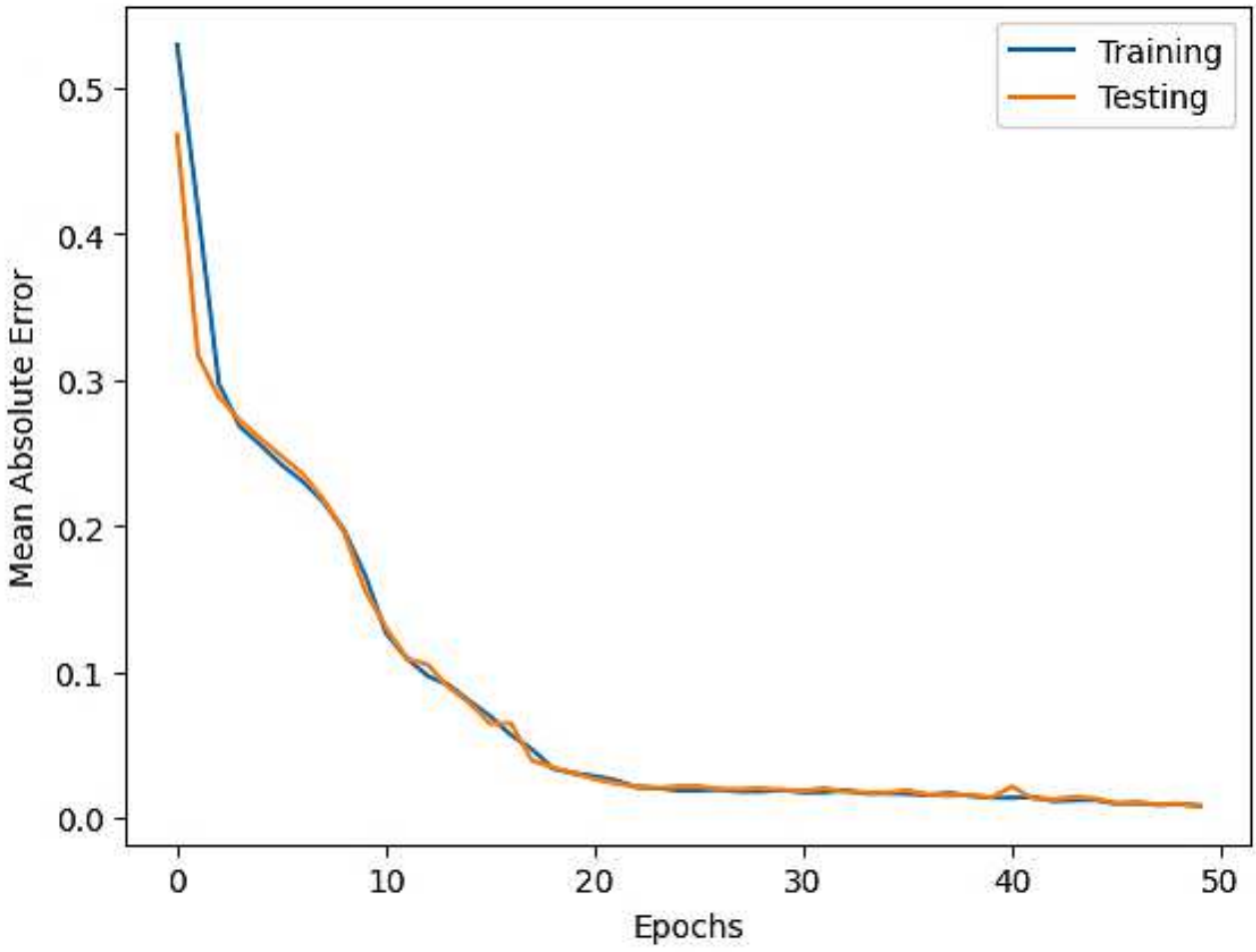

Fig. 5: Learning and testing curve. The mean squared absolute error as a function of the running epochs for the CNN-BRNN model used in forecasting climate temperature.

architecture is demonstrated in Figure 4 that are based on the given configuration:
Input Layer: The input to the model is a sequence of vectors, where each vector has a length of 14 for the first dataset and 23 for the second dataset. The input shape is (1, 14, 1) for the first dataset and (1, 23, 1) for the second dataset.
Convolutional Layers: 128 filters with a kernel size of 10 and make up the first convolutional layer. 64 filters with a kernel size of 7 comprise the second convolutional layer. 16 filters with a kernel size of 5 make up the third convolutional layer. All convolutional layers use the ReLU activation function.
Max-Pooling Layer: After the third convolutional layer, a max-pooling layer with 2x2 size is applied to reduce spatial dimensions of the input.
BRNN Layer: max-pooling layer's output is utilized in a bidirectional recurrent neural network layer with 256 hidden units. The BRNN layer uses the LSTM cell.
Fully Connected Layer: A fully connected layer of 64 neurons receives the output of the BRNN layer and applies the ReLU activation function.
Output Layer: The linear activation function is used in the output layer and consists of one neuron.
The sigmoid function is utilized as the output layer's activation function. The model's batch size is 64 with 0.001learning rate, Adam optimizer, 48-time steps, and 50 epochs. The pseudocode of the proposed CNN-BRNN model is described in Algorithm 1. The strength of the proposed method is that, by incorporating CNN and BRNN, the model exploits the strengths of both architectures. The CNN efficiently extracts spatial features, while the BRNN component captures temporal dependencies, leading to a comprehensive understanding of the data and improving the process of the prediction. The weakness of the proposed method is that the model is computational complexity, because incorporating CNN and BRNN requires more processing power and large

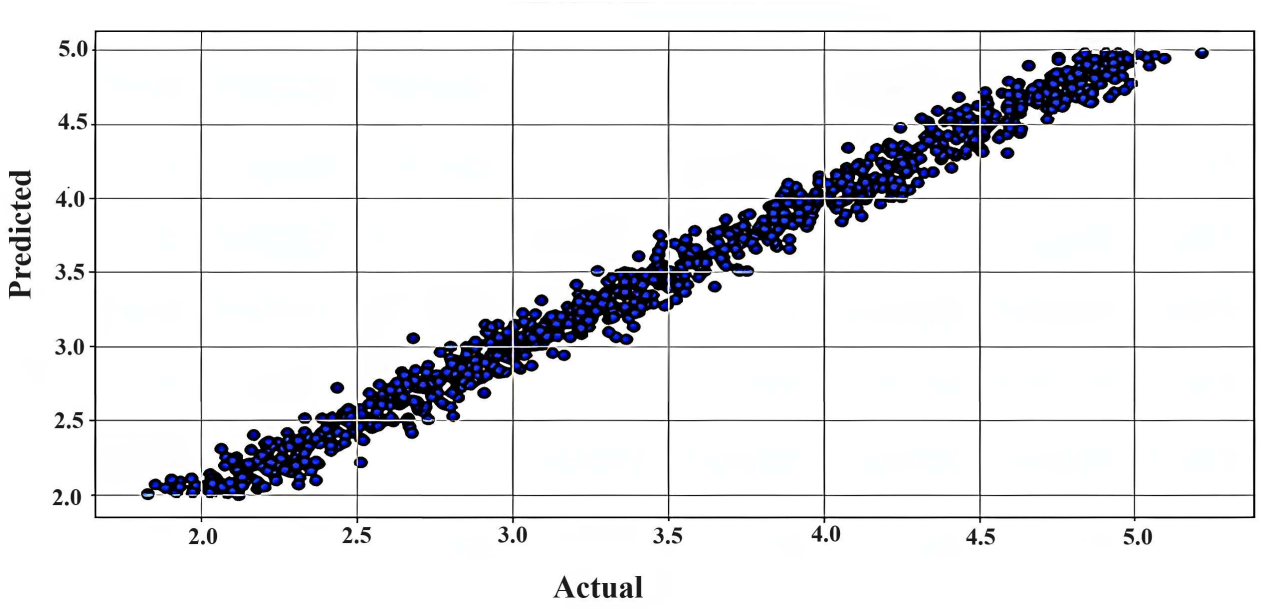

Fig. 6: Actual temperature vs estimated temperature for CNN-BRNN.

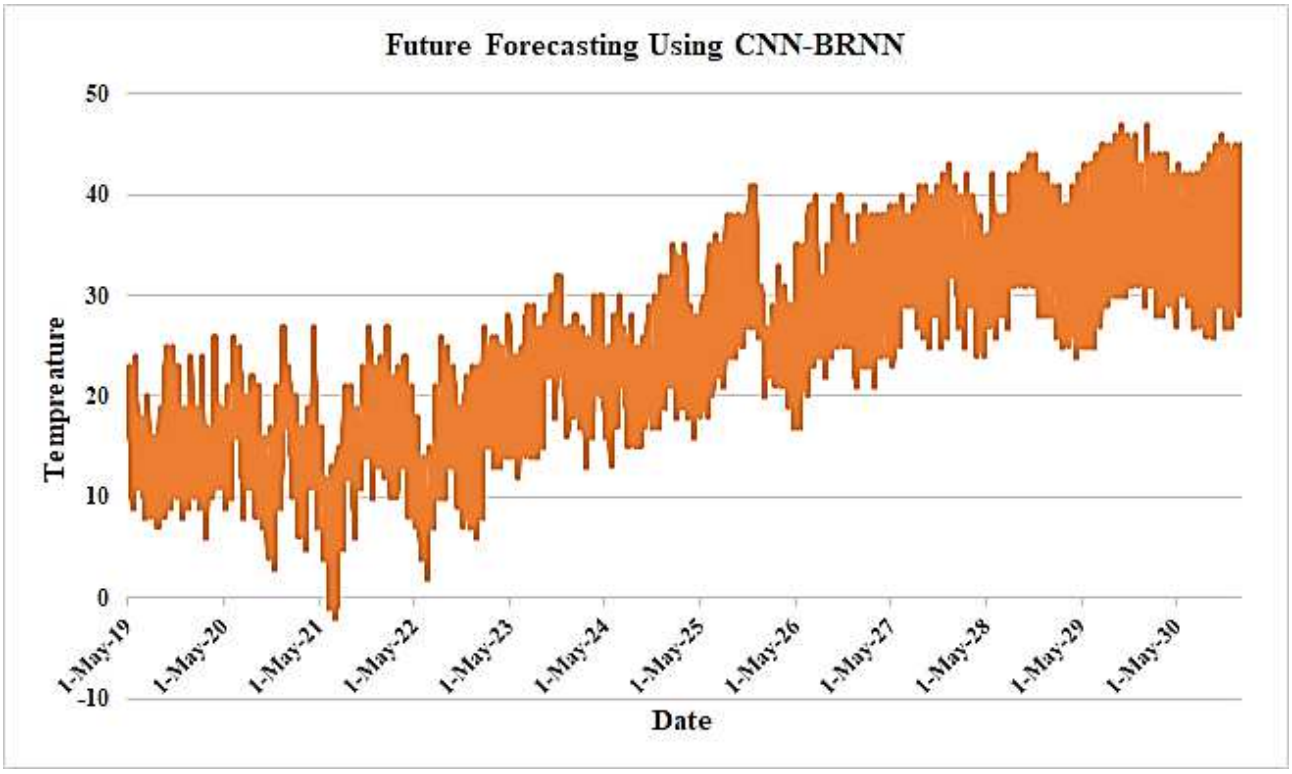

Fig. 7: Future temperature prediction until 2030 using the CNN-BRNN model.

memory. Also, due to the model complex, this can lead to overfitting.

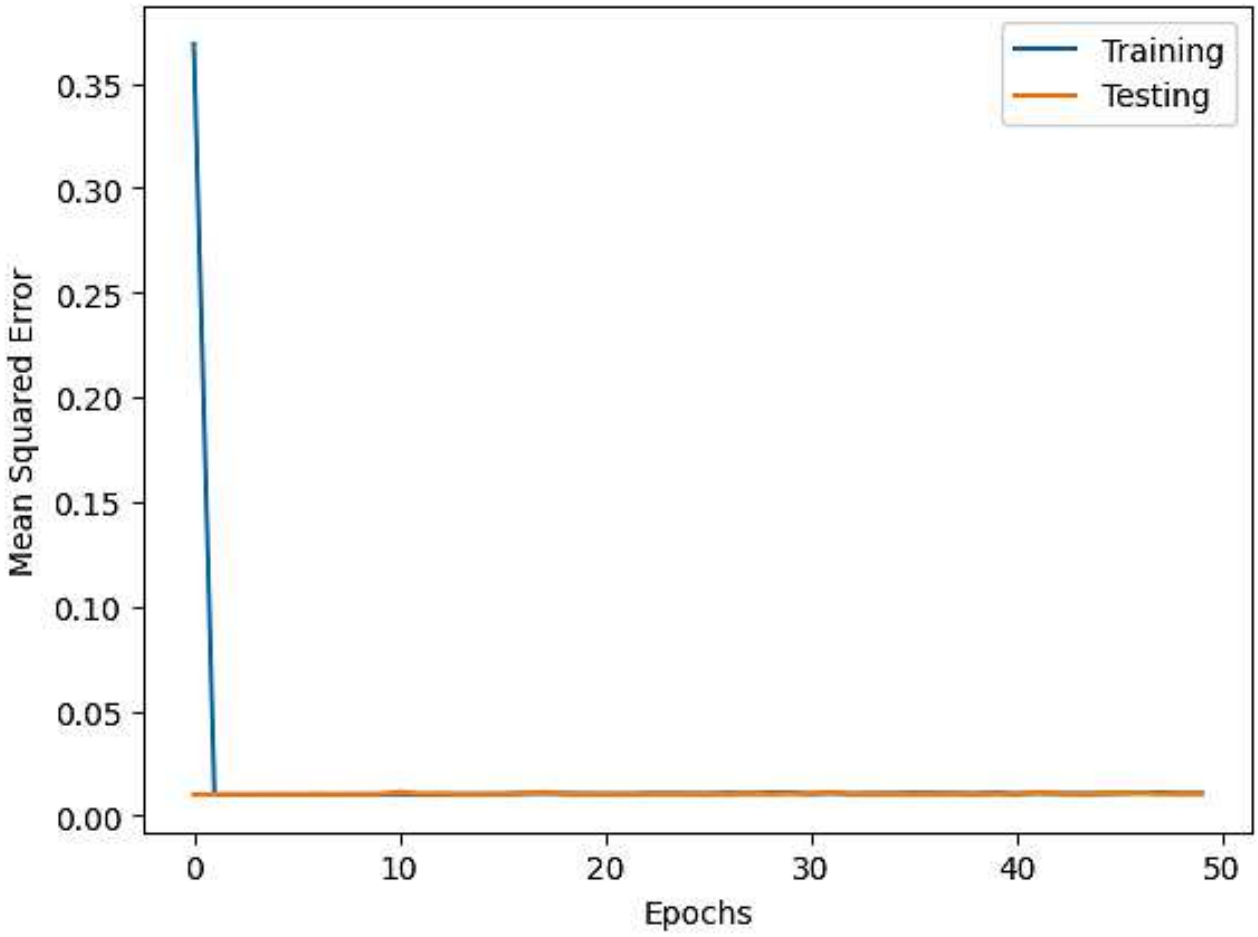

Fig. 8: The learning and testing curves. The mean squared absolute error as a function of the running epochs for the CNN-BRNN model used in forecasting climate sea level pressure.

Table 3: Evaluation metrics for assessing the proposed approach.

Metric Name	Metric Abbreviation	Value
Mean Absolute Error	MAE	$\frac{1}{n}\sum_{i=1}^{n}\lvert Pre_i - Act_i\rvert$
Mean Square Error	MSE	$\frac{1}{n}\sum_{i=1}^{n}(Pre_i - Act_i)^2$
Root Mean Square Erro	RMSE	$\sqrt{\frac{1}{n}\sum_{i=1}^{n}(Pre_i - Act_i)^2}$
Median Absolute Error	MedAE	$median(\lvert Pre_1 - Act_1\rvert, \ldots, \lvert Pre_n - Act_n\rvert)$
Coefficient of determination	R^2	$R^2 = 1 - \frac{\sum_{i=1}^{n}(Act_i - Pre_i)^2}{\sum_{i=1}^{n}(\sum_{i=1}^{n}(Act_i) - Act_i)^2}$

3.3.2 Random Forest (RF) Regressor

Using a collection of trees is the optimal method for enhancing the predictive accuracy of decision trees. Random Forest refers to a set of regression trees that are constructed in a random manner. The Random Forest Regressor is well-suited for real-time applications across several areas, including language modeling [52], bioinformatics [53], species distribution modeling [54], and ecological modeling [55]. The dataset is divided into subgroups and several decision trees are trained. The final outcomes are determined by majority voting, where the outcomes are averaged. Thus, when compared to XGBoost and ANN, RF was demonstrated to be the most effective methodology through bootstrap aggregation and replacement techniques [56].

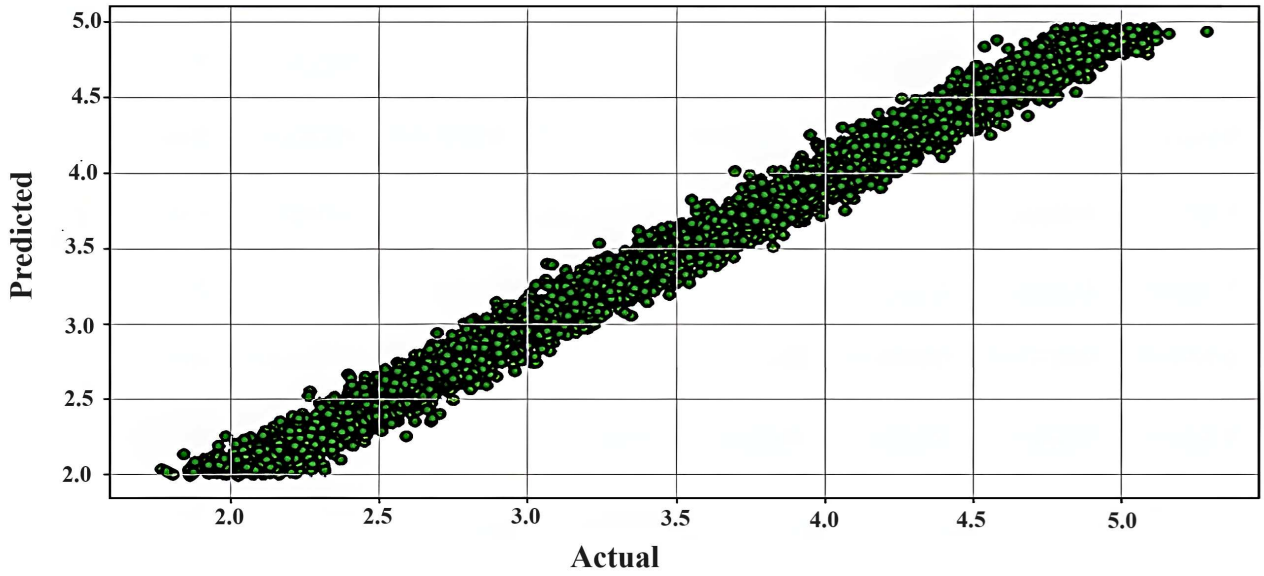

Fig. 9: Actual atmospheric sea level pressure vs predicted atmospheric sea level pressure for CNN-BRNN performance.

Table 4: Hyperparameters for the five traditional machine learning regression models.

Models	Hyperparameters
RF	Trees number in the random forest is No. of estimators = 10.
Knn	KNN Neighbors number is No.neighbors= 5. The "distance" weight function is used, which assigns weights to neighbors based on their distance.
SVR	The tolerance for stopping criteria during training is $Tol = 0.001$. The regularization parameter is $C = 1$. The kernel is "rbf" (Radial Basis Function).
DR	The training set prediction is set to mean, so Strategy = "mean".
GB	The learning rate for gradient boosting is 0.00001. The number of boosting stages is 50. The maximum depth of the individual regression estimators is 2.

Table 5: The proposed CNN-BRNN model and the regression models outcomes for predicting the temperature using the first dataset.

Model	MSE	MAE	MedAE	RMSE	R^2
CNN-BRNN	1.27×10^{-05}	0.0022	0.0014	0.0034	99.61%
RF	0.0024	0.0066	0.0051	0.0072	95.17%
KNN	0.0030	0.0070	0.0058	0.0079	94.76%
SVR	0.0041	0.0077	0.0061	0.0082	92.59%
GB	0.0046	0.0079	0.0065	0.0085	91.26%
DR	0.0050	0.0083	0.0067	0.0090	90.88%

Table 6: The proposed CNN-BRNN model and the regression models outcomes for predicting atmospheric sea level pressure using the second dataset.

Model	MSE	MAE	MedAE	RMSE	R^2
CNN-BRNN	0.0103	0.0818	0.0639	0.1019	98.61%
RF	0.0355	0.0950	0.0735	0.2478	94.29%
KNN	0.0388	0.0976	0.0779	0.2731	93.56%
SVR	0.0421	0.1829	0.0833	0.3677	93.22%
GB	0.0458	0.2271	0.0869	0.3919	92.71%
DR	0.0510	0.2627	0.0919	0.4318	91.98%

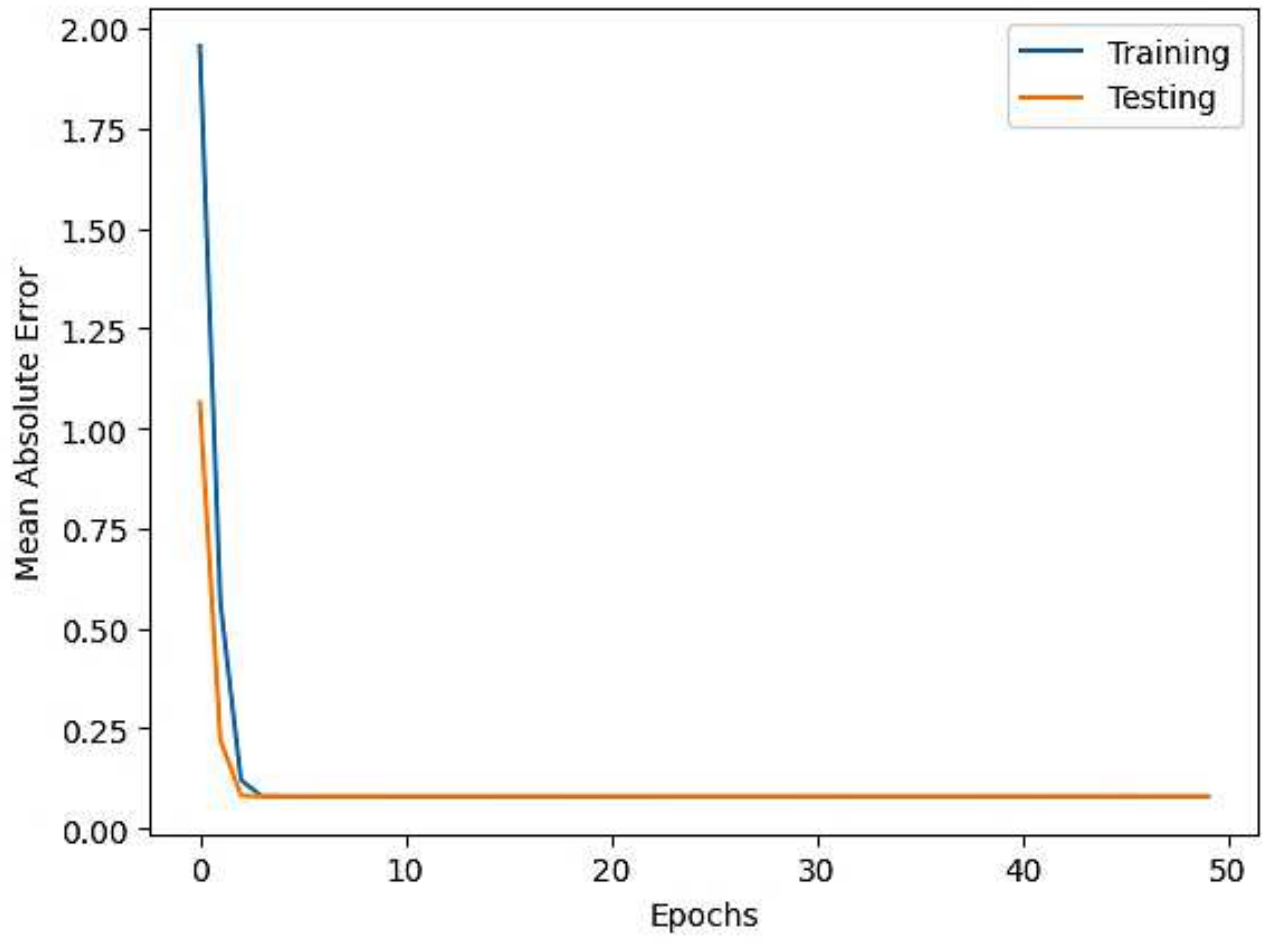

Fig. 10: The learning and testing curves. The mean absolute error as a function of epochs number for the CNN-BRNN model used in forecasting climate visibility distance prediction.

Table 7: The proposed CNN-BRNN model and the regression models outcomes for predicting visibility distance using the second dataset.

Model	MSE	MAE	MedAE	RMSE	R^2
CNN-BRNN	0.0100	0.0807	0.0688	0.1009	98.73%
RF	0.0428	0.0973	0.0769	0.2861	94.20%
KNN	0.0449	0.0990	0.0812	0.3414	93.39%
SVR	0.0534	0.2624	0.0856	0.3859	92.96%
GB	0.0559	0.2811	0.0885	0.4192	92.70%
DR	0.0591	0.3183	0.0912	0.4468	92.06%

3.3.3 K-Nearest Neighbor (KNN) Regressor

KNN is an instant-based learning approach where the function is assessed, and all computations are deferred until the classification stage. For regression issues, the variable's value can be conveyed to regular KNN values using the same procedure. This method may be employed to assess the significance of contributions made by neighboring individuals, with closer neighbors having a greater influence on the average outcome compared to more distant ones. In a regression issue, the prediction is ascertained by computing The mean of the results of the nearest neighbors [57].

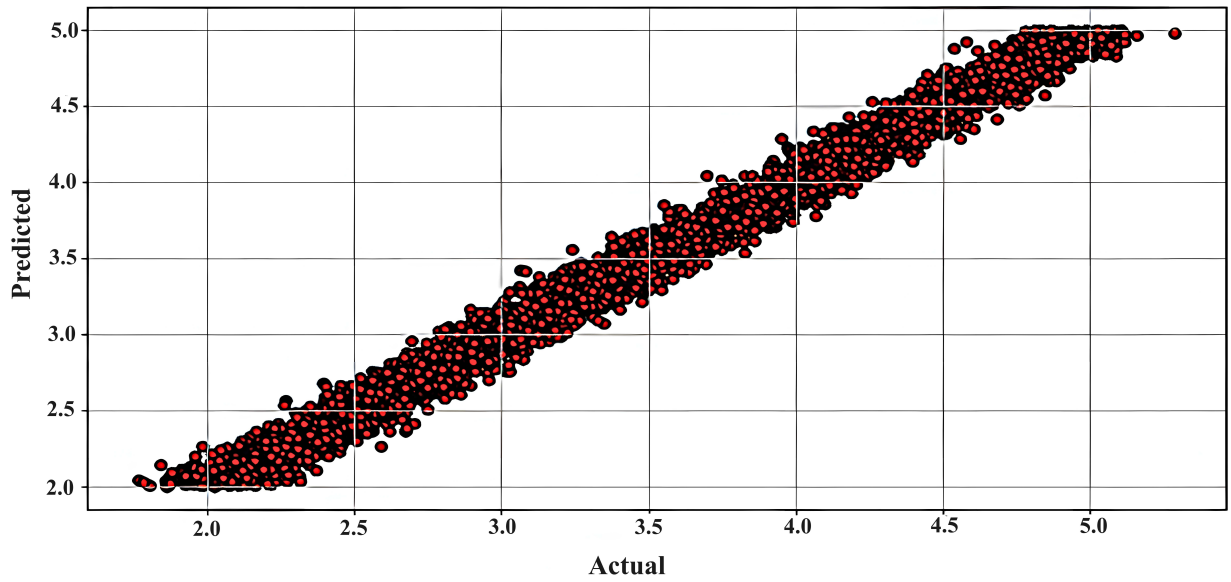

Fig. 11: Actual visibility distance vs predicted visibility distance for CNN-BRNN performance.

Table 8: The proposed CNN-BRNN model and the regression models outcomes for predicting air temperature dew point using the second dataset.

Model	MSE	MAE	MedAE	RMSE	R^2
CNN-BRNN	0.0098	0.0798	0.0681	0.0999	98.67%
RF	0.0348	0.0925	0.0733	0.2486	94.88%
KNN	0.0378	0.0951	0.0756	0.2751	94.62%
SVR	0.0413	0.0979	0.0791	0.3159	94.29%
GB	0.0553	0.1265	0.0825	0.3568	94.02%
DR	0.0579	0.1645	0.0858	0.3811	93.75%

3.3.4 Support Vector Regressor (SVR)

The support vector machine is a prevalent data mining technology utilized for classification and pattern identification. SVM has notable characteristics such as significant performance in dealing with non-linear data, enhanced efficacy in high-dimensional domains, and the capability to generalize [58]. In order to assess the linear relationship between the multi-dimensional inputs and the one-dimensional output, the Support Vector Regression (SVR) method seeks to transform the input data into a high-dimensional feature space and identify the best hyperplane. This allows for solving non-linear problems in a space with many dimensions [59]. The ideal hyperplane is determined only by a restricted training data set referred as the support vectors. These support vectors are the sample data that meet the boundary requirement [60]. Incorporating an explanation of kernel functions and their role in SVR enhances the understanding of how the model operates and its ability to handle complex data relationships. In SVR, the process of converting input data into a high-dimensional feature space and identifying an optimal hyperplane to assess the linear relationship between multi-dimensional inputs and a one-dimensional output is facilitated by the use of kernel functions. Kernels are mathematical functions that allow SVR to implicitly map the input data into a space with more dimensions, where it might be more easily separated or approximated by a hyperplane. Commonly used kernels in SVR include polynomial, linear, sigmoid kernels, and radial basis function (RBF) [61]. Among these, the RBF kernel is particularly popular due to its capacity to represent intricate, nonlinear relationships between input and output variables. The input data points are mapped onto a higher-dimensional space, where a linear relationship could be more obvious, using a kernel that computes the similarity between them in the original space. By leveraging appropriate kernels, SVR effectively models nonlinear relationships in the data while still benefiting from the mathematical framework of linear regression in the higher-dimensional feature space. Through this procedure, SVR is able to determine which

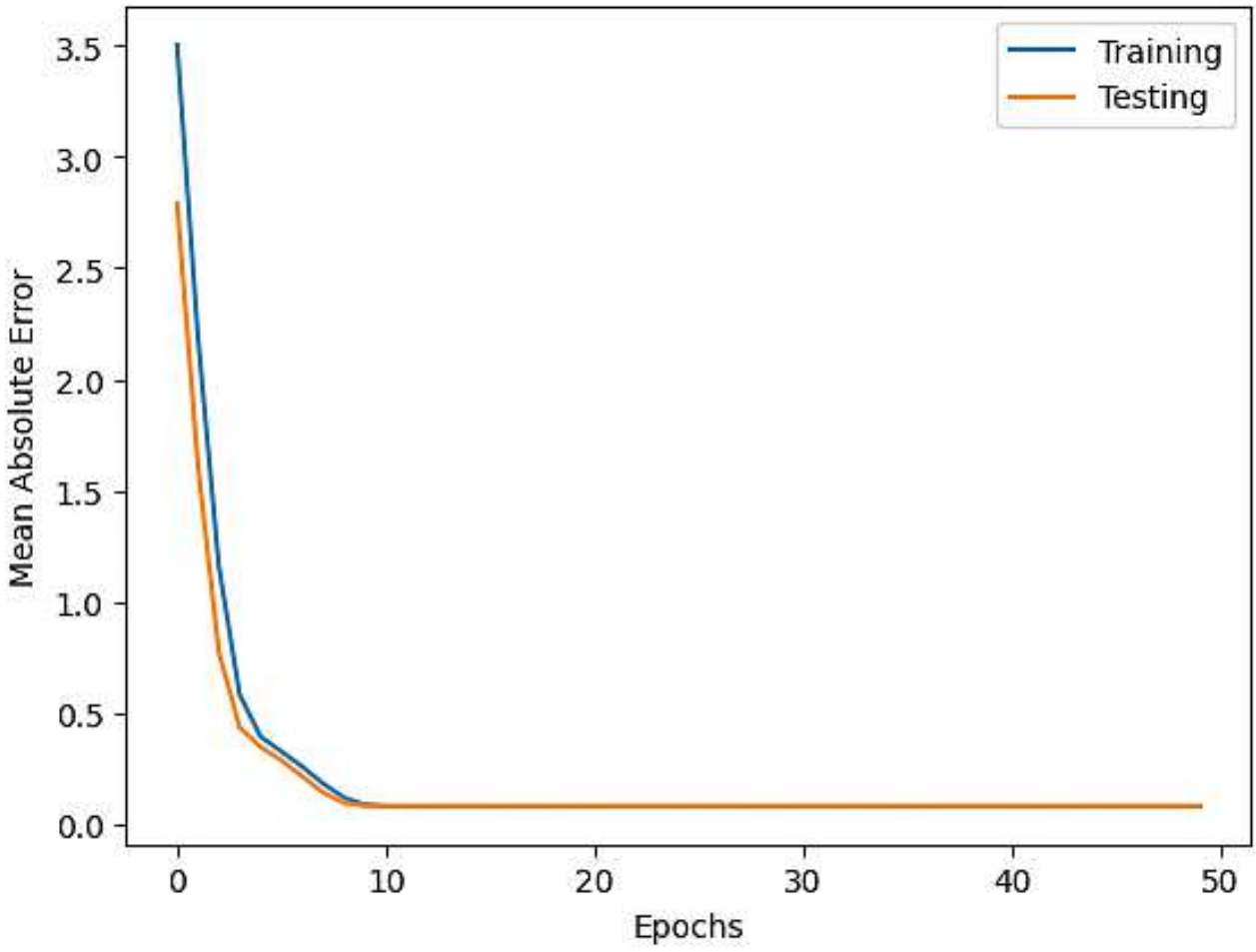

Fig. 12: The learning and testing curves as a function of the mean absolute error in epochs number of the running epochs for the CNN-BRNN model used in forecasting the presence of dew in the air temperature climate.

hyperplane best fits the training set and has the best generalization to new data points [62].

3.3.5 Gradient Boosting (GB) Regressor

GB is an ML algorithm [63] that builds a strong classifier for regression and classification applications by combining many weaker classification techniques, frequently decision trees. The system is constructed incrementally, similar to previous methods of boosting, and is made more generalized by making the most of a suitable cost function. In GB approach, misclassified cases in one phase are assigned greater importance with high weight for the subsequent step. The advantages of GB encompass rapid processing and high predictive accuracy. This strategy has a strong resemblance to Adaptive Boosting, but with the disadvantage of bad influence on outliers and overwhelmed by noisy data [**?**].

3.3.6 Gradient Boosting (GB) Regressor

DR technique is often regarded as a standard method because to its reliance on straightforward criteria to accomplish prediction. The foundation for forecasting can be derived from either user-determined constants or the median, quantile and mean, of the training set. It functioned as a benchmark for assessing other models. In order to utilize dummy parameters, it is necessary to transform nominal data. The dummy parameter serves as a numerical indication for different subsamples, in regression analysis. A dummy variable is used to indicate the presence of more than unique treatment groups in the research design. A dummy variable is used to assign a binary value of 1 to subjects that belong to the interest group while subjects in the comparative group are assigned a value of 0 [31,64].

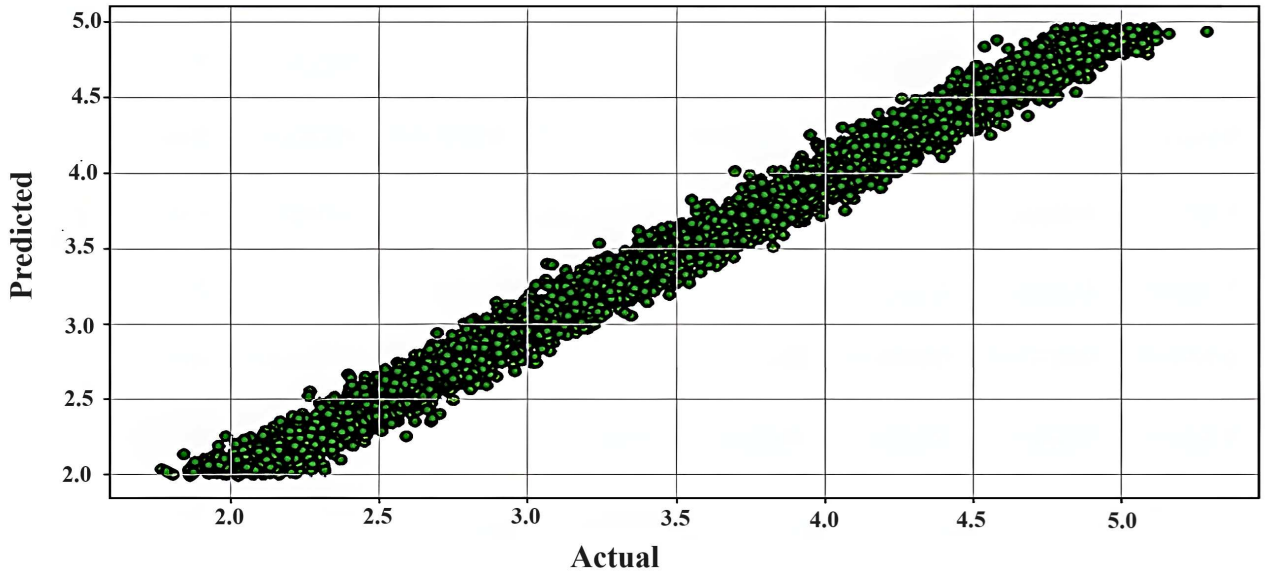

Fig. 13: Actual air temperature dew point vs predicted air temperature dew point for CNN-BRNN performance.

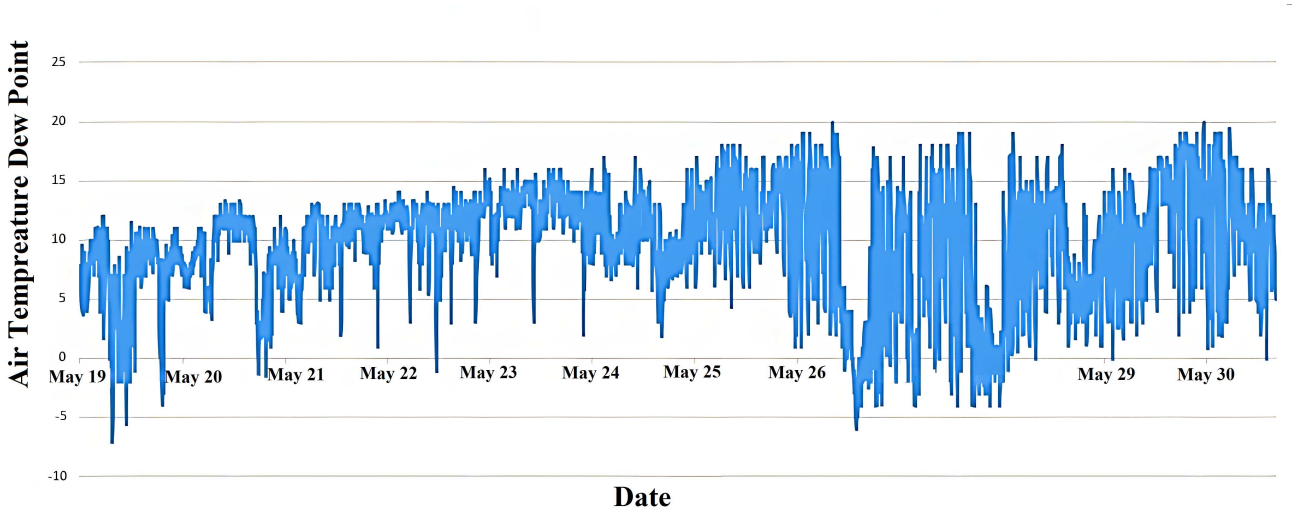

Fig. 14: Future air temperature dew point prediction until 2030 using the CNN-BRNN model.

3.3.7 Evaluation metrics

The proposed CNN-BRNN model is evaluated using performance measurements [25,26,65] as illustrated in Table 3. where n denotes the dataset sample size, and Act_i, pre_i are the i^{th} actual and predicted values.

4 Experimental and Results

Jupyter Notebook version 6.4.6 is used for executing the experiments in this paper. It is a powerful environment for creating, conducting, and recording experiments. It supports several computer languages, including Python 3.8. All experiments are conducted on the same platform, with Intel Core i5 processor, 16 GB storage capacity, and Microsoft Windows 10 PC. In these experiments, we introduce a deep learning model named CNN-BRNN, and its performance is compared against five traditional machine learning models: RF, KNN, SVR, GB, and DR. To evaluate the models, we employed five metrics that are explained in Table 3. The experiments are conducted using two datasets, one for predicting future temperatures up to 2030 and another for predicting three climate predictions —namely, atmospheric sea level pressure,

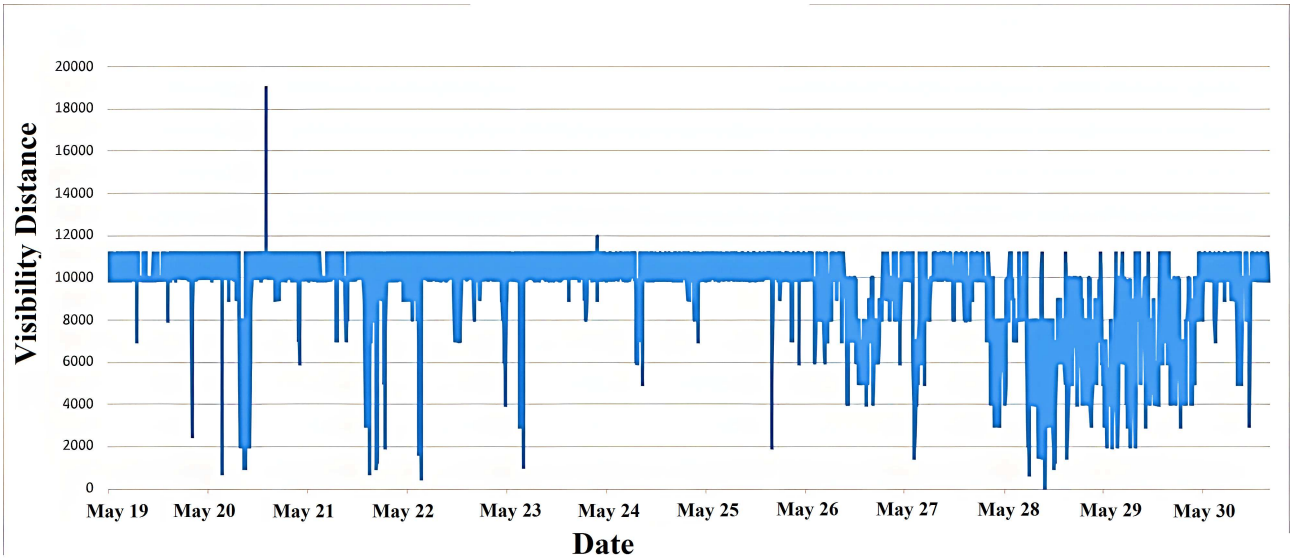

Fig. 15: Future visibility distance until 2030 using the CNN-BRNN model.

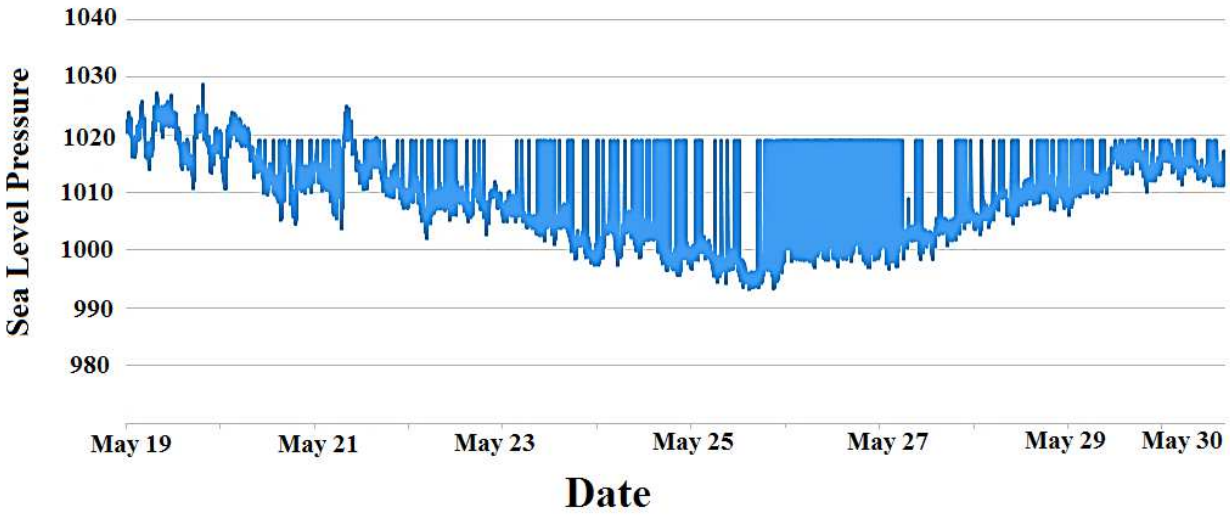

Fig. 16: Future atmospheric seal level pressure until 2030 using the CNN-BRNN model.

visibility distance, and air temperature dew point. These predictions are made using the proposed model. The topology of the proposed CNN-BRNN model comprises an input layer, three convolutional layers, single max-pooling layer, single bidirectional recurrent neural network layer, fully connected layer and one output layer. There are 128 filters in the first convolution layer, and the kernel size is 10. The second convolutional layer consists of 64 filters and a kernel size of seven. The third convolutional layer consists of 16 filters and a kernel size of five. The 2x2 max-pooling layer is used to minimize the input's spatial dimensions. There are 256 hidden units in the BRNN layer. A fully connected layer of 64 neurons receives the output of the BRNN layer and applies the ReLU activation function. In the output layer, the sigmoid function is used as the activation function. The optimizer used for the model is Adam optimizer; the batch size is 64; the number of epochs is 50; the learning rate is 0.001. Benchmarking the proposed CNN-BRNN model against the five classical ML regression models (RF, SVR, KNN, GB, and DR) yields comparable performance results. Hyper parameter values for these models are presented in Table 4, outlining the specific details for each regression model employed in this research. Table 5 presents the

Algorithm 1 Pseudocode of CNN-BRNN

```
Initialize the CNN-BRNN architecture.
for iteration = 1 to the number of iterations do
    Initialize the training data population.
    for batch = 1 to the number of batches do
        // Forward Pass
        Initialize the input array for each convolutional layer.
        for i = 1 to 3 do
            Apply convolution operation to the first convolutional layer using 128 filters and a kernel size of 10, the second layer using 64 filters and a kernel size of 7, and the third convolutional layer using 16 filters and a kernel size of 5.
            Apply activation function (ReLU).
            if Max Pooling is enabled for the current layer then
                Apply max pooling operation with a step size of 2 and a pool size of 2.
            end if
        end for
        Flatten the output of the convolutional layers.
        Pass the flattened output to the BRNN layer with 256 hidden units.
        Pass the output of the BRNN layer to the dense layer with 64 neurons.
        Apply activation function (ReLU).
        Pass the dense layer's output to the output layer.
        Update the weights and biases of the network using the Adam optimizer.
        // Backward Pass
        Compute the loss between the actual and the predicted output.
        Compute the loss function's gradients in relation to the weights and biases.
        Adjust the network's weights and biases using the gradients.
    end for
end for
// Test the model's accuracy
for each test sample in the test dataset do
    // Forward Pass
    Pass the test sample to the input layers of the CNN-BRNN architecture.
    Perform the same operations as during the training phase for each layer in the network.
    Calculate the predicted output.
    Compare the expected output with the actual output for the test sample.
end for
Return the proposed CNN-BRNN architecture accuracy.
```

performance evaluation outcomes for the CNN-BRNN model and five traditional ML regression models (RF, SVR, KNN, GB, and DR) in predicting temperature for the first dataset, using metrics defined in Table 3. The CNN-BRNN model fared better than the other regression models, with the lowest MAE, MSE, RMSE, MedAE, and the highest R2 at 0.0022, 1.27x10-05, 0.0034, 0.0014, and 99.61%, respectively. In contrast, the DR model exhibited the least favorable results, with higher values for MSE (0.0050), MAE (0.0083), MedAE (0.0067), RMSE (0.0090), and R2 (90.88%). These metrics results assert outperformance predictive performance of the proposed CNN-RNN model compared to the other models. Figure 5 demonstrates the learning and testing curves consist of two plots. The left curve illustrates the mean absolute error as a function of epochs number. On the other side, the right curve depicts the mean squared absolute error as a function of the running epochs for the CNN-BRNN model used for predicting the temperature using the first dataset. It is evident from these curves that this model generalizes its learned experience well. Consequently, the performance of the suggested CNN-BRNN model with both the expected and real temperatures is shown in Figure 6. It is notoriously obvious from Figure 6 that this model generalized the unseen data reliably which reveals the accurate prediction of temperature readings. Table 6 outlines the findings of the CNN-BRNN model's performance evaluation along with those of five conventional ML regression models (KNN, RF, SVR, GB, and DR) in predicting atmospheric sea level pressure based on wind speed rate and air temperature for the second dataset. The performance metrics reported in Table 3 are used to evaluate these models. The CNN-BRNN model outperformed the other regression models, obtaining the greatest R2 and the lowest MAE, MSE, MedAE, and RMSE at 98.61%, 0.0818, 0.0103, 0.0639, and 0.1019, respectively. In contrast, the DR model exhibited less favorable results, with higher values for MSE (0.0510), MAE (0.2627), MedAE (0.0919), RMSE (0.4318), and R2 (91.99%). These findings highlight the effectivness of the proposed CNN-BRNN model in predicting atmospheric sea level pressure in comparison to traditional regression models. Figure 7 shows the future prediction of temperature to 2030 using the CNN-BRNN model. Figure 8 demonstrates the learning and testing curves consist of two plots. The left curve illustrates the mean absolute error as a function of the epochs number. The right curve depicts the mean squared absolute error as a function of the running epochs for the CNN-BRNN model used for predicting the atmospheric sea level pressure using the second dataset. The proposed CNN-BRNN model's performance is shown in Figure 9 using the actual atmospheric sea level pressure and the predicted atmospheric sea level pressure. As demonstrated in Figure 9 this model generalized the unseen data reliably which indicates the accurate estimation of temperature values. Table 7 presents the outcomes of performance evaluation for the CNN-BRNN model alongside five traditional machine learning regression models (RF, KNN, SVR, GB, and DR) in predicting visibility distance based on air temperature, wind speed rate, and atmospheric sea level pressure for the second dataset. The evaluation utilized various performance metrics defined by Table3. In comparison to the other regression models, the

CNN-BRNN model performed better, obtaining the lowest MAE, MSE, MedAE, RMSE, and the greatest R2 at 0.0807, 0.0100, 0.0688, 0.1009, and 98.73%, respectively. Conversely, the DR model displayed less favorable results, with higher values for MSE (0.0591), MAE (0.3183), MedAE (0.0912), RMSE (0.4468), and R2 (92.06%). These results highlight the effectiveness of the proposed CNN-BRNN model in predicting visibility distance compared to traditional regression models. Figure 10 demonstrates the learning and testing curves, which consist of two plots. The left curve illustrates the mean absolute error as a function of epochs number. In contrast, the right curve depicts the mean squared absolute error as a function of the running epochs for the CNN-BRNN model used to predict the visibility distance using the second dataset. Figure 11 illustrates the the proposed CNN-BRNN model performance using the actual visibility distance and the predicted visibility distance. Figure 11 illustrates the visibility distance values were accurately predicted. Table 8 presents the outcomes of the performance assessment for the CNN-BRNN model and five traditional machine learning regression models (RF, KNN, SVR, GB, and DR) in predicting air temperature dew point based on air temperature, wind speed rate, atmospheric sea level pressure, and visibility distance for the second dataset. Table 3 provides an explanation of the performance metrics that were used in the evaluation. In comparison to the other regression models, the CNN-BRNN model performed better, obtaining the lowest MAE, MSE, MedAE, RMSE, and the greatest R2 at 0.0798, 0.0098, 0.0681, 0.0999, and 98.67%, respectively. In contrast, the DR model displayed less favorable results, with higher values for MSE (0.0579), MAE (0.1645), MedAE (0.0858), RMSE (0.3811), and R2 (93.75%). These findings emphasize the effectiveness of the CNN-BRNN model in predicting air temperature dew point compared to traditional regression models. Figure 12 demonstrates the learning and testing curves consist of two plots. The left curve illustrates the mean absolute error as a function of epochs number. While the right curve depicts the mean squared absolute error as a function of the running epochs for the CNN-BRNN model used for predicting the air temperature dew point using the second dataset. Figure 13 illustrates the performance of the proposed CNN-BRNN model using the actual air temperature dew point and the predicted air temperature dew point. Figure 13 is fitted to a line which revealed the accurate prediction of the air temperature dew point values. Using the future prediction results of temperature up to 2030 (as explained in Figure 7), an additional experiment was executed to predict the air temperature dew point using the proposed CNN-BRNN model. The results of this experiment are detailed in Figure 14. Furthermore, another experiment was conducted to predict the visibility distance up to 2030, based on the future prediction results of temperature which explained in Figure 7 and the air temperature dew prediction which is explained in Figure 14. The outcomes of this experiment are presented in Figure 15. Lastly, a final experiment was carried out to forecast the atmospheric sea level pressure up to 2030, utilizing the future prediction results of temperature that is explained in Figure 7, air temperature dew which is explained in Figure 14, and visibility distance that is explained in Figure 15. The results of this experiment are highlighted in Figure 16. The obtained results shows that the CNN-BRNN model predicts that the temperature in May 2030 in Saudi Arabia will average 45 degrees, compared to the current average of 25 degrees. Therefore, this anticipated result projects an increase of 20 degrees in the spring season of 2030. In the second scenario, it is evident from Figure 14 that the CNN-BRNN model predicts that the average rate of the air temperature dew point prediction will increase on the interval May 2026 to May 2030 in Saudi Arabia compared to the interval May 2019 to May 2023. In the third scenario, it is obvious from Figure 15 that the CNN-BRNN model predicts that the average air visibility distance will decrease abnormally in the Saudi Arabia from May 2026 to May 2030 compared to the period from May 2019 to May 2025. Finally, in the final scenario, it is evident from Figure 16 that the CNN-BRNN model predicts that the average atmospheric sea level pressure will decrease in the Saudi Arabia from May 2024 to May 2028 compared to the period from May 2019 to May 2023. Then, it will increase to be close to the average normal level.

5 Conclusion

The goal of sustainable development is to satisfy present demands without sacrificing the capacity of future generations to satisfy their own. It entails taking into account how our actions affect the environment and making choices that advance long-term well-being. This paper discussed a deep learning model that predicts temperature, air temperature dew point, visibility distance, and air pressure at sea level. These factors are crucial for implementing a sustainable climate change adaptation plan and contributing to the achievement of Vision 2030's production and energy efficiency goals. The study aimed to combine various ocean-atmospheric factors using ML and DL techniques to anticipate climate changes in temperature, atmospheric sea level pressure, visibility distance, and air temperature dew point. Evaluation metrics were employed to assess the models' effectiveness. When compared to five other ML regressors (Support Vector, Random Forest, K-Nearest Neighbor, Gradient Boosting, and Dummy regressor), CNN-BRNN outperforms them. The deep learning model that is utilized in this work is a combination of BRNN and CNN, trained on four future climate predictions using two datasets. The results demonstrate that integrating ocean and atmospheric data through a hybrid CNN and BRNN approach enhances climate change prediction across all future climate predictions.

Acknowledgement

Acknowledgment: This project is sponsored by Prince Sattam Bin Abdulaziz University (PSAU) as part of funding for its SDG Roadmap Research Funding Programme project number PSAU/2023/SDG/88.

References

[1] Allen, M., Dube, O. P., Solecki, W., Aragón-Durand, F., Cramer, W., Humphreys, S., ... & Zickfeld, K., Global warming of 1.5 C. An IPCC Special Report on the impacts of global warming of 1.5 C above pre-industrial levels and related global greenhouse gas emission pathways, in the context of strengthening the global response to the threat of climate change, Sustain. Dev. Efforts to Eradicate Poverty, (2018).

[2] M. Zidan, A. M. Eisa, M. Qasymeh and M. A. I. Shoman, A Quantum Algorithm for System Specifications Verification, IEEE Internet of Things Journal **11(14)**, 24775-24794 (2024).

[3] M. Zidan, A. -H. Abdel-Aty, A. Khalil, M. Abdel-Aty and H. Eleuch, "A Novel Efficient Quantum Random Access Memory, IEEE Access **9**, 151775-151780 (2021).

[4] M. Zidan, M.G. Eldin, M. Y. Shams, A. Abd-Elhamed,M. Abdel-Aty, A quantum algorithm for evaluating the hamming distance, Computers, Materials & Continua. **71(1)**, 1065–1078 (2022).

[5] W. Liu, B. Wang, J. Fan, Y. Ge, M. Zidan, A quantum system control method based on enhanced reinforcement learning, Soft Computing **26(14)**, 6567-6575 (2022).

[6] L. Yu, S. Qin, M. Zhang, C. Shen, T. Jiang, and X. Guan, A review of deep reinforcement learning for smart building energy management, IEEE Internet of Things Journal **8(15)**, 12046–12063 (2021).

[7] M. Kazemian and B. Shafei, Carbon sequestration and storage in concrete: A state-of-the-art review of compositions, methods, and developments, J. CO2 Util. **70**, 102443 (2023).

[8] J.-P. Lai, Y.-M. Chang, C.-H. Chen, and P.-F. Pai, A survey of machine learning models in renewable energy predictions, Appl. Sci. **10(17)**, 5975 (2020).

[9] S. Padmanaban, M. A. Nasab, T. Samavat, M. Zand, and M. A. Nasab, Artificial Intelligence techniques for smart power systems, IoT and Analytics in Renewable Energy Systems **1**, 107–123 (2023).

[10] F. Golpayegani, S. Ghanadbashi, A. Zarchini, Advancing Sustainable Manufacturing: Reinforcement Learning with Adaptive Reward Machine Using an Ontology-Based Approach, Sustainability **16(14)**, 5873 (2024).

[11] J. Bharadiya, Artificial intelligence in transportation systems a critical review, Am. J. Comput. Eng. **6(1)**, 34–45 (2023).

[12] F. K. Shaikh, M. A. Memon, N. A. Mahoto, S. Zeadally, and J. Nebhen, Artificial intelligence best practices in smart agriculture, IEEE micro. **42(1)**, 17–24 (2021).

[13] K. P. Tran, Artificial intelligence for smart manufacturing: Methods and applications, Sensors **21(16)**, 5584 (2021).

[14] I. Md Jelas, M. A. Zulkifley, M. Abdullah, and M. Spraggon, Deforestation detection using deep learning-based semantic segmentation techniques: a systematic review, Front. For. Glob. Chang. **7**: 1300060 (2024).

[15] S. Saravi, R. Kalawsky, D. Joannou, M. Rivas Casado, G. Fu, and F. Meng, Use of artificial intelligence to improve resilience and preparedness against adverse flood events, Water **11(5)**, 973 (2019).

[16] P. A. Owusu and S. Asumadu-Sarkodie, A review of renewable energy sources, sustainability issues and climate change mitigation, Cogent Eng. **3(1)**, 1167990 (2016).

[17] S. Cevik, Climate change and energy security: the dilemma or opportunity of the century?, Environ. Econ. Policy Stud. **26**, 653–672 (2024).

[18] L. Chen, Z. Chen, Y. Zhang, Y. Liu, A. I. Osman, M. Farghali, J. Hua, A. Al-Fatesh, I. Ihara, D. W. Rooney, P.-S. Yap, Artificial intelligence-based solutions for climate change: a review, Environmental Chemistry Letters **21**, 2525–2557 (2023).

[19] H. S. Kang, J. Y. Lee, S. Choi, H. Kim, J. H. Park, J. Y. Son, B. H. Kim, S. D. Noh, Smart manufacturing: Past research, present findings, and future directions, Int. J. Precis. Eng. Manuf. Technol. **3**, 111–128 (2016).

[20] L. A. Bewoor, A. Bewoor, and R. Kumar, Artificial intelligence for weather forecasting, Artificial Intelligence, CRC Press., 231–239 (2021).

[21] Z. Cheng, M.-S. Pang, and P. A. Pavlou, Mitigating traffic congestion: The role of intelligent transportation systems, Inf. Syst. Res. **31(3)**, 653–674 (2020).

[22] A. Zahoor, T. Xu, M. Wang, M. Dawood, S. Afrane, Y. Li, J. L. Chen, G. Mao, Natural and artificial green infrastructure (GI) for sustainable resilient cities: A scientometric analysis, Environ. Impact Assess. Rev. **101**, 107139 (2023).

[23] A. Zahoor, T. Xu, M. Wang, M. Dawood, S. Afrane, Y. Li, J. L. Chen, G. Mao, Natural and artificial green infrastructure (GI) for sustainable resilient cities: A scientometric analysis, Environ. Impact Assess. Rev. **101**, 107139 (2023).

[24] L. Helsen, Tackling Climate Change with Machine Learning, ACM Computing Surveys **55(2)**, 1-96 (2022)

[25] W. Leal Filho, T. Wall, S. A. R. Mucova, G. J. Nagy, A. L. Balogun, J. M. Luetz, , ... & O. Gandhi, Deploying artificial intelligence for climate change adaptation, Technol. Forecast. Soc. Change. **180**, 121662 (2022).

[26] A. Kern, Z. Barcza, H. Marjanović, Tamás Árendás, N. Fodor, P. Bónis, P. Bognár, J. Lichtenberger, Statistical modelling of crop yield in Central Europe using climate data and remote sensing vegetation indices, Agric. For. Meteorol. **260**, 300–320 (2018).

[27] B. Bochenek, Z. Ustrnul, Machine learning in weather prediction and climate analyses—applications and perspectives, Atmosphere (Basel) **13(2)**, 180 (2022).

[28] T. Brahimi, Using artificial intelligence to predict wind speed for energy application in Saudi Arabia, Energies **12(24)**, 4669 (2019).

[29] B. Acharya, S. Dey, M. Zidan, IoT-Based Smart Waste Management for Environmental Sustainability, CRC Press, 1-196 (2022).

[30] S. Idowu, R. Schmidpeter, N. Capaldi, L. Zu, M. Del Baldo, and R. Abreu, Encyclopedia of sustainable management, Springer Cham, 1-4003 (2020).

[31] A. M. Elshewey, M. Y. Shams, A. M. Elhady, S. M. Shohieb, A. A. Abdelhamid, A. Ibrahim, Z. Tarek, A Novel WD-SARIMAX Model for Temperature Forecasting Using Daily Delhi Climate Dataset, Sustainability. **15(1)**, 757 (2022).

[32] J. Bartok, A. Bott, M. Gera, Fog prediction for road traffic safety in a coastal desert region, Boundary-layer Meteorol. **145**, 485–506 (2012).
[33] M. Ahmadi, A. Gholizadeh Lonbar, M. Nouri, A. Sharifzadeh Javidi, A. Tarlani Beris, A. Sharifi, A. Salimi-Tarazouj, Supervised multi-regional segmentation machine learning architecture for digital twin applications in coastal regions, J. Coast. Conserv. **28(2)**, 44 (2024)
[34] A. Sharifi, A. T. Beris, A. S. Javidi, M. S. Nouri, A. G. Lonbar, and M. Ahmadi, Application of artificial intelligence in digital twin models for stormwater infrastructure systems in smart cities, Adv. Eng. Informatics. **61**, 102485 (2024).
[35] A. A. Awosusi, N. G. Xulu, M. Ahmadi, H. Rjoub, M. Altuntaş,S. E. Uhunamure, ..., D. Kirikkaleli, The sustainable environment in Uruguay: the roles of financial development, natural resources, and trade globalization, Front. Environ. Sci. **10**, 875577 (2022).
[36] S. Jafarzadeh-Ghoushchi, A. Sharifi, M. Ahmadi, and M. Maghami, Statistical study of seasonal storage solar system usage in Iran, J. Sol. Energy Res. **2(3)**, 39–44 (2017).
[37] J. Artin, A. Valizadeh, M. Ahmadi, S. A. P. Kumar, and A. Sharifi, Presentation of a novel method for prediction of traffic with climate condition based on ensemble learning of neural architecture search (NAS) and linear regression, Complexity **2(3)**, 1–13 (2021).
[38] P. Mahyawansi, S. R. Zanje, A. Sharifi, D. McDaniel, and A. S. Leon, Experimental and numerical investigation of a small scale storm sewer geyser, J. Hydraul. Res. **62(1)**, 25–38 (2024).
[39] S. P. Nitsure, S. N. Londhe, and K. C. Khare, Prediction of sea water levels using wind information and soft computing techniques, Appl. Ocean Res. **47**, 344–351 (2014).
[40] R. TÜR, E. Tas, A. Haghighi, A. Mehr, Sea level prediction using machine learning, Water **13(24)**, 3566 (2021).
[41] M. Baljon and S. K. Sharma, Rainfall prediction rate in Saudi Arabia using improved machine learning techniques, Water **15(4)**, 826 (2023).
[42] S. Alawadi, D. Mera, M. Fernández-Delgado, F. Alkhabbas, C. M. Olsson, P. Davidsson, A comparison of machine learning algorithms for forecasting indoor temperature in smart buildings, Energy Syst. **13**, 689–705 (2022)
[43] C. M. Liyew, H. A. Melese, Machine learning techniques to predict daily rainfall amount, J. Big Data **8**, 1–11 (2021).
[44] C. Nyasulu, A. Diattara, A. Traore, A. Deme, C. Ba, Towards Resilient Agriculture to Hostile Climate Change in the Sahel Region: A Case Study of Machine Learning-Based Weather Prediction in Senegal, Agriculture. **12(9)**, 1473 (2022).
[45] Z. Tarek, A. M. Elshewey, S. M. Shohieb, A. M. Elhady, N. E. El-Attar, S. Elseuofi, M. Y Shams, Soil Erosion Status Prediction Using a Novel Random Forest Model Optimized by Random Search Method, Sustainability **15(9)**, 7114(2023).
[46] Z. Tarek, M. Y. Shams, S. K. Towfek, H. K.Alkahtani, A. Ibrahim, A. A. Abdelhamid, M. M. Eid, N. Khodadadi, L. Abualigah, D. S. Khafaga, A. M. Elshewey, An Optimized Model Based on Deep Learning and Gated Recurrent Unit for COVID-19 Death Prediction, Biomimetics. **8(7)**, 552 (2023).
[47] M. Gabor, R. Zdunek, Compressing convolutional neural networks with hierarchical Tucker-2 decomposition, Applied Soft Computing. **132**, 109856 (2023).
[48] L. Zhu, P. Spachos, E. Pensini, K. N. Plataniotis, Deep learning and machine vision for food processing: A survey, Curr. Res. Food Sci. **4**, 233–249 (2021).
[49] Q. Sun, S. Lee, and D. Batra, Bidirectional beam search: Forward-backward inference in neural sequence models for fill-in-the-blank image captioning,IEEE Conference on Computer Vision and Pattern Recognition, 6961–6969 (2017).
[50] M. Dhyani, R. Kumar, An intelligent Chatbot using deep learning with Bidirectional RNN and attention model, Mater. today Proc. **34**, 817–824 (2021).
[51] Z. Wang, Y. Li, X. He, R. Yan, Z. Li, Y. Jiang, X. Li, Improved deep bidirectional recurrent neural network for learning the cross-sensitivity rules of gas sensor array, Sensors Actuators B Chem. **401**, 134996 (2024).
[52] P. Xu, F. Jelinek, Random forests and the data sparseness problem in language modeling, Comput. Speech Lang. **21(1)**, 105–152 (2007).
[53] A. S Sakr, M. Shams, A. Mahmoud, M. Zidan, Amino acid encryption method using genetic algorithm for key generation, Comput Mater Contin **70(1)**, 123-134 (2022).
[54] A. Sagheer, M. Zidan, M. M. Abdelsamea, A novel autonomous perceptron model for pattern classification applications, Entropy **21(8)**, 763 (2018).
[55] S. M. Simon, P. Glaum, F. S. Valdovinos, Interpreting random forest analysis of ecological models to move from prediction to explanation, Sci. Rep. **13(1)**, 3881 (2023).
[56] M. Y. Shams, Z. Tarek, A. M. Elshewey, M. Hany, A. Darwish, A. E. Hassanien, A Machine Learning-Based Model for Predicting Temperature Under the Effects of Climate Change, in The Power of Data: Driving Climate Change with Data Science and Artificial Intelligence Innovations, Springer., 61–81 (2023).
[57] Y. K. Saheed, R. M. Ayobami, T. Orje-Ishegh, A Comparative Study of Regression Analysis for Modelling and Prediction of Bitcoin Price, in Blockchain Applications in the Smart Era, Springer., 187–209 (2022).
[58] M. Asadi, K. Pourhossein, Modeling and Siting of wind farms using Support Vector Regression (SVR), International Aegean Conference on Electrical Machines and Power Electronics (ACEMP) and International Conference on Optimization of Electrical and Electronic Equipment (OPTIM), IEEE., 511–516 (2019).
[59] C. Niu, K. Tan, X. Jia, X. Wang, Deep learning based regression for optically inactive inland water quality parameter estimation using airborne hyperspectral imagery, Environ. Pollut. **286**, 117534 (2021).
[60] X. Nong, C. Lai, L. Chen, D. Shao, C. Zhang, J. Liang, Prediction modelling framework comparative analysis of dissolved oxygen concentration variations using support vector regression coupled with multiple feature engineering and optimization methods: A case study in China, Ecol. Indic. **146**, 109845 (2023).
[61] B. Schölkopf, A. Smola, and K.-R. Müller, Kernel principal component analysis, in International conference on artificial neural networks, Springer, 583–588 (1997).
[62] A. J. Smola, B. Schölkopf, A tutorial on support vector regression, Stat. Comput. **14**, 199–222 (2004).
[63] A. Natekin, A. Knoll, Gradient boosting machines, a tutorial, Front. Neurorobot. **7(21)**, 2013.

[64] M. Hubert, P. J. Rousseeuw, Robust regression with both continuous and binary regressors, Journal of Statistical Planning and Inference **57(1)**, 153-163 (1997)
[65] M. A. Al-Betar, S. Kassaymeh, S. N. Makhadmeh, S. Fraihat, S. Abdullah, Feedforward neural network-based augmented salp swarm optimizer for accurate software development cost forecasting, Applied Soft Computing. **149**, 111008 (2023).
[66] A. Escamilla-García, G. M. Soto-Zarazúa, M. Toledano-Ayala, E. Rivas-Araiza, A. Gastélum-Barrios, Applications of artificial neural networks in greenhouse technology and overview for smart agriculture development, Appl. Sci. **10(11)**, 3835 (2020).

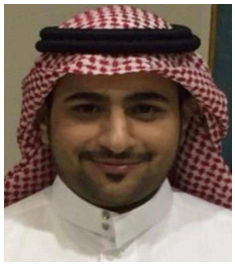

FAHAD ALJUAYDI received the M.S. degree in Mathematics from the Florida Institute of Technology, Florida, USA, and Ph.D. degree in Mathematics from the Curtin University Perth, WA, Australia. He has been a assistant professor of mathematics with Prince Sattam bin Abdulaziz University, Saudi Arabia, He has authored or coauthored more than 10 articles. His research interests include applied mathematics and mathematical physics, including different directions in Convolutional Neural Network,Flow Velocity,Hidden Layer, Highway Traffic Flow, Learning Algorithms,Learning Models, Long Memory, Long Short-term Memory, Machine Learning, Machine Learning Models. He has refereed articles for more than 5 journals of physics and mathematics.

Bikash K. Behera received the dual B.S.–M.S. degrees from the Indian Institute of Science Education and Research (IISER) Kolkata, Mohanpur, India, in 2018.He is currently the Founder, the CEO, and the Director of Bikash's Quantum Private Ltd., Mohanpur. His research interests include quantum machine learning, quantum optimization, quantum communication, and quantum simulation.

AHMED M. ELSHEWEY is an Associate Professor of Computer Science and Artificial Intelligence at Faculty of Computers and Information, Suez University, Egypt. He received the B.Sc. degree in Computer Science in 2007 from Mansoura University, M.Sc. degree in Computer Science in 2014 from Zagazig University, and Ph.D. degree in Computer Science in 2017 from Damietta University. He has published over 31 articles in international journals. His research interests include Artificial Intelligence, Data Science, Data Mining, Optimization, Machine Learning and Deep Learning.

ZAHRAA TAREK Zahraa Tarek received B.Sc. degree in Computer Science from the University of Mansoura, Egypt, in 2009, and M.Sc in Computer Science from Mansoura University in 2015. In 2015, she joined, as assistant teacher, the Department of Computer Science, Mansoura University, and in 2017 she registered as a PhD research student in computer science department at faculty of computer and information system in the same university. She obtained the Ph.D. degree in Computer Science from the Faculty of Computers and Information in 2019. She has published many publications till now. Her research interests include Cloud Computing, Internet of Things, Fog Computing, Blockchain, Machine Learning, Software Engineering, Deep Learning, Regression models, Grid Search, Optimization Algorithms, Intelligent Systems, Smart Cities, Swarm Optimization, Genetic Algorithm, Fuzzy Theory, Classification, Supervised Learning, Scheduling, Load Balancing, Neural Networks and Artificial Intelligence, Pattern Recognition, Classification, Unsupervised Learning, Feature Extraction and Selection, Prediction, Machine Intelligence, Fuzzy Clustering, Predictive Modeling and Analytics, Medical Diagnosis, Face Recognition, Metaheuristic, Fuzzy Logic, Evolutionary Computation, Bio-Inspired Computing, Cybersecurity.